NTNU
Norwegian University of
Science and Technology

Mass Forecasting of Similar-Behaving Neighbor Dry Gas Shale Wells

Vegard Haugstvedt

Petroleum Geoscience and Engineering
Submission date: March 2017
Supervisor: Curtis Hays Whitson, IGP

Norwegian University of Science and Technology
Department of Geoscience and Petroleum

Abstract

Shale gas production in the US is steadily increasing. With the increase in drilled production wells comes the increased demand for reliable and cost-effective well production forecasts.

Decline curves like the Arps (1945) rate equation is frequently applied to shale wells for forecasting purposes. However, due to the ultra-low rock permeabilities in unconventional wells, one may experience an absence of depletion type flow during a well history. This leads to the curve-fitting of transient data, which can yield unreasonably positive production forecasts.

History matching of wells to numerical models using reservoir simulators is considered perhaps to be the most reliable and effective tool for shale well production forecasting, provided that enough information on the reservoir, fluid and completion is at hand. This method is widely used, but neglected by some, due to the cost, time and information that is needed to perform the procedure.

The purpose of this work has been to combine the two concepts, by proposing a workflow that can yield reliable forecasts at a relatively low cost and that requires only information on rates and tubing pressures for most wells. This thesis tests a procedure that forecasts multiple neighboring, similarly-completed shale gas wells with the signature of a single, representative, history matched well.

Specifically, a unique group behavior is identified by observing well signatures in a log-log plot of pseudo-pressure drawdown normalized rate versus material balance time, and in a Specialized linear flow plot, along with historical production and pressure plots. A unique group behavior is identified by identifying similar flow regimes, their duration and overall well behavior. A representative well of the group is subsequently forecasted with a history-matched numerical model. The forecast signature of the pseudo-pressure drawdown normalized rate derivative with respect to material balance time is applied to the remaining wells and adjusted to follow the historical data trajectory. A group of five real, similarly performing wells is examined and forecasted with the procedure. The forecast results are compared to the forecasts of each wells' unique history matched model for comparison.

The procedure succeeds in producing reasonable forecasts for the entire group, and all results are close to the respective history matched model forecasts.

The study is in its essence empirical and the number of wells examined is limited to five. A broader study comprising more wells is suggested for future work. Further, quantifying how much the well, reservoir and completion parameters in the group can differ, while still produce reasonable forecasts with the procedure, is another interesting problem and not investigated in this work.

Sammendrag

Produksjonen av skifergass i USA er stadig økende. Med et voksende antall borede produksjonsbrønner, skapes det naturlig nok et større behov for brønnproduksjonsprognoser.

Nedgangskurver, slik som Arps' rate-ligning er ofte brukt i industrien til å predikere fremtidig brønnproduksjon. Metoden er enkel, koster ingenting og er derfor populær. Dog, denne metoden kan fort overpredikere en skiferbrønns framtidige produksjon. På grunn av de ultra-lave verdiene for skifer-permeabilitet, vil grensedominert strømning ikke forekomme før etter lang tids produksjon. Dette bidrar til at man tilpasser rate-kurven til transient strømning, noe som kan føre til altfor positive langtidsprognoser.

Konstruksjon av historietilpassede numeriske modeller med reservoarsimulatorer, er en annen metode for å predikere fremtidig produksjon og er ansett som en mer pålitelig metode og i henhold til fysiske grunnprinsipper. Metoden er mye brukt men ofte satt til side, på grunn av investeringen av tid, penger og informasjon som en historietilpasset numerisk modell krever.

Målet med dette arbeidet har vært å kombinere de to konseptene, ved å foreslå en prosedyre som kan produsere pålitelige produksjonsprediksjoner for en billigere penge og som trenger kun informasjon om produksjonsrater og tubing-trykkdata for de fleste brønner. En metode har blitt prøvd som kan produsere produskjonsprognoser for en gruppe skifergassbrønner som produserer fra samme formasjon og komplettert på en lik måte, ved å lage en historietilpasset modell for én representativ brønn.

En unik gruppe-oppførsel blant brønnene identifiseres ved å sammenligne datasignaturene til de ulike brønnene i log-log-plottet til pseduotrykk-normalisert rate mot materialbalansetid, samt i lineær strømnings-plottet og i vanlige rate- og trykkprofiler mot tid. En unik gruppeoppførsel identifiseres ved å se etter like strømningsregimer, deres varighet og generell oppførsel.

Produksjonen til en brønn som er ansett som representativ for gruppeoppførselen blir predikert med en historietilpasset numerisk modell. Signaturen til den predikerte brønnen blir brukt til å lage prognoser for fremtidsproduksjonen til de resterende brønnene. Fem ekte brønner fra Haynesville-formasjonen ble predikert med metoden og samtidig sammenlignet med historietilpassede numeriske modeller for hver enkelt brønn. Prosedyren bidro til å produsere fornuftige prognoser for alle brønner i gruppen, og alle resultater ligger tett til prognosene laget av de historietilpassede numeriske modellene.

Dette er en empirisk studie som begrenser seg til undersøkelse av fem brønner. En bredere studie som omfatter mer data er foreslått som et framtidig arbeid. Videre vil det være interessant å kvantifisere hvor mye reservoar- og kompletteringsparametre kan variere for de ulike brønnene, men fortsatt produsere fornuftige prognoser med den undersøkte metoden.

Acknowledgements

First and foremost, I would like to thank my supervisor Curtis. H. Whitson, for his support throughout this work. His guidance and care has been very much appreciated.

I would also like to thank all the professors and students at IPT that have made me enjoy the student life throughout the last years. Last but not least, I want to thank friends and family and my parents especially, for their endless support throughout the years.

Contents

List of Figures

List of Tables

1. Introduction

For the last decade, gas production from shale in the US has skyrocketed and is today a big contributor to the annual US gas production. With the increases in production and number of drilled wells, so too increases the demand for reliable well production forecasts.

Decline Curve Analysis (DCA), like the Arps (1945) rate equation, and other, modified versions, are used widely in the industry for predicting future well performance. Because of the Arps rate equations' simplicity, it can be used to provide forecasts quickly and virtually without cost. The Arps rate equation and others are also applied to shale well performance prediction. However, due to the nature of the ultra-low permeability shale formations, there is often an absence of full depletion-type flow for an entire well production history. The Arps equation is the then curve-fitted to transient data. The procedure can thus lead to overly positive performance predictions.

History Matched well models, using reservoir simulators based on the diffusivity equation, is another procedure for producing well forecasts. Governed by the equations that describe fluid flow through porous media, this method is in accordance with basic theory. The challenge for this approach is the number of reservoir and completion parameters that must be known to accurately describe the reservoir and its fluid flow. For shale, many parameters like rock permeability and porosity are difficult to determine. Important parameters like relative permeability exponents are assumed to have values like conventional reservoirs because of the difficulty in deriving these values for shale. A simple, symmetrical geometry is often assumed, as the only information available is data on the completion procedure. The result is often the construction of a model that is probably far from what the reservoir look like downhole, but a good-fit history matched model can represent the reservoir in a decent way. Along with analytical solutions, numerical modeling is the most correct way to perform forecasts, as it is rooted in the physics that govern flow though porous media.

The downside of creating forecasts based on history-matched models, is the time and cost that must be invested. To create history matched numerical models for every well in an area is costly and require detailed completion and reservoir data for each well. To construct history matched models for every well in a confined area might not be necessary to perform reliable forecasts. The latter assertion is the motivation behind this work.

This work consists of six chapters. The second chapter covers background on the concepts that are used in the proposed procedure or that is at some level relevant to mention. The third chapter

discusses the pseudo-pressure normalized decline curve versus material balance time derivative, m_{mb}, which is used in the forecasting procedure. The fourth chapter describes the forecasting procedure step by step. The fifth chapter presents the forecast results for five real wells producing from the same formation, generated with the procedure described in chapter three. The last chapter provides conclusions and suggestions to further work.

2. Background

2.1 Decline Curve Analysis (DCA) and Forecasting

Decline Curve Analysis is the analysis of declining production rates and the forecasting of future performance of oil and gas wells. The decline in oil and gas production is usually a function of time, loss of reservoir pressure or change of relative volume of the produced fluid(s). The basis of the concept is fitting a curve to a wells' performance history and then assume that the same trend will continue in the future, given that the production trend is stable and that production conditions are not changed in the future. The basic assumption is that the causes that controlled the curve trend during the well history, will continue to govern the trend in the future, in a uniform manner.

Arps (1945) collected these ideas and presented empirically rooted equations for decline rate analysis based on open hole oil wells producing under constant well pressure conditions. The equations were derived for oil wells, but can also be applied to gas producing wells. The functions can be expressed as

$$\frac{1}{D} \equiv -\frac{q}{dq/dt} \quad \text{.....(2.1)}$$

$$b \equiv \frac{d}{dt}\left[\frac{1}{D}\right] \equiv -\frac{d}{dt}\left[\frac{q}{dq/dt}\right] \quad \text{.....(2.2)}$$

and are called the nominal decline and the "Arps b", respectively. If the nominal decline D is constant, it yields the exponential decline rate equation and can be shown to be

$$q = \frac{q_i}{e^{Dt}} \quad \text{.....(2.3)}$$

where q is the current producing rate and q_i is the initial rate of the curve-fit. D is the constant nominal decline.

When the nominal decline is not constant, and b is shown, or assumed to be, constant and above zero, the hyperbolic rate decline equation is obtained and given as

$$q = \frac{q_i}{(1+bD_it)^{1/b}} \quad \text{.....(2.4)}$$

where D_i is the initial nominal decline of the curve-fit.

Fetkovich (1980, 1983) demonstrated that the Arps decline equations (hyperbolic and exponential) are applicable for a wide range of oil and gas wells with a constant flowing bottomhole pressure and during boundary-dominated flow. He applied the constant pressure solution to the diffusivity equation and showed that exponential decline is boundary-dominated flow in a closed reservoir producing an incompressible single phase liquid, at a constant flowing pressure with the "open hole" condition, thus demonstrating that DCA is more than empirical curve fitting. A b > 0 was tied to recovery mechanisms for higher-compressible and multiphase fluid systems.

Because of their simplicity, the Arps rate equations are still widely used in the industry as a production forecasting tool, over 70 years after being published.

The equations have also been applied to tight gas sand and shale (unconventional) reservoirs, which have often lead to overestimation of reserves. This is because the curve fits are done when full depletion has not yet commenced. Unconventional wells are often observed to have very long periods of transient flow contribution. By curve-fitting historical, transient data, very high b-values are obtained which leads to overestimation of the ultimate recovery. As a response to this, several different modifications to the Arps equations have been proposed in the literature to prevent unrealistically high figures, like the power-law nominal decline of Ilk et Al. (2008), which forces exponential decline at a specified time.

Reese et Al. (2014) evaluated the Arps parameters during the full history for both field and synthetic cases of planar fracture shale dry gas wells under the assumption of constant flowing pressures. For a planar fracture model geometry with evenly spaced, identical hydraulic fractures with infinite fracture conductivity, where reservoir extent was defined by the fracture half-length x_f, a b-value of 2 was observed during linear flow, and a b-value ranging between 0 and 0.5 was observed during complete depletion. These values agree with previous findings by Fetkovich. For models with a reservoir extent greater than the fracture half-length, a b-value over 2 was observed during linear flow, and a b between 0.5 and 1 during depletion. The increased b-value is linked to the transient flow contribution from the unstimulated matrix beyond the fracture tips. It was also emphasized that there was a significant period of time between the end of linear flow and the occurrence of a minimum b-exponent. This corresponds to the fact that unstimulated shale reservoirs have very low values of the hydraulic rock diffusivity constant, which governs how quickly a pressure wave moves through the reservoir rock. The result is that a very long transient period is observed.

2.2 Numerical Modeling and Forecasting

In this work, the commercial simulator SENSOR© is used for all simulation purposes. The integrated asset modeling software Pipe-It© is used for automatizing the process of history matching.

Numerical well modeling by simulators based on the diffusivity equation is widely used as a tool for shale reservoir fluid modeling and production forecasting. A numerical model of a shale well can be constructed, provided there is sufficient data on the well completion, produced fluid and the reservoir. A reservoir geometry is determined based on the well completion procedure. Data on produced fluid, rates and tubing pressures is gathered. For a dry gas well, tubinghead pressures can easily be converted into flowing pressures with an empirical correlation, like the Gray Correlation (1978). A Black Oil table is constructed based on the dry gas specific gravity and the reservoir temperature.

Ideally, production diagnostic plots should be examined to ensure that the geometry and fracture assumptions made for the numerical model agree with the regime signature observed in the plot.

Typically, a set of reservoir parameters are unknown when constructing the numerical shale well model, like matrix permeability, fracture half-length (if reservoir geometry assumes planar fractures), water saturation, relative permeability exponents etc. The values for the set of unknown parameters are altered so that the numerical model bottomhole pressure values match the calculated bottomhole pressure values of the historical data. This is the procedure known as History Matching. Normally, a forecast is then produced by running the history-fitted model for a longer period, e.g. 30 years. An obvious basic forecast would produce the forecast based on a constant flowing pressure from the last day in history. Several forecasts can be produced with different pressure profiles.

An advantage of current reservoir simulators, is their ability to easily include nonlinearities caused by pressure dependent rock and fluid parameters. A special case for fractured wells is the possible scenario that fractures are pressure sensitive. When reservoir pore pressure drops and effective overburden stress increases, it creates the possibility that fractures fully or partially close. In this work, when the effect is applied during history-matching, the relationship that is used to calculate pressure dependent fracture permeability is

$$\frac{k}{k_0} = 10^{m\left(\frac{p-p_i}{p_{ref}}\right)} \quad \text{.....(3.1)}$$

Where k and k_0 are the current and initial fracture permeability, p is the current bottomhole pressure, p_i is the initial reservoir pressure and p_{ref} is some reference pressure (default at 1000 psi), all in consistent units. m is the dimensionless slope of the pressure dependent permeability relationship.

Another concept that is particular for shale gas reservoirs, is adsorbed gas. Adsorption is the phenomenon where gas accumulate on the surface of organic material in the rock, existing in a condensed, near liquid state. As pressure drops, some of the gas desorbs and becomes free gas. In the simulator, the black-oil table is modified to include adsorbed gas. The effect is accounted for by defining a small, immobile oil saturation. The amount of gas dissolved in the oil is calculated from the Langmuir equation[1] and a gas-oil ratio relationship[2].

It is important to mention that a range of different history matches, each converged on a different set of values for the unknown parameters, can be equally accurate in reproducing the historical rate and flowing pressure data. A single history match is merely one possible version of the well. A long well production history is preferred as this can limit the range of potentially good history matches. Ideally, multiple history matches, each converging on a different set of parameter values should be conducted to identify the value ranges for key reservoir parameters. When each of the history matched models are then forecasted, it will yield a range of possible values of ultimate recovery.

The often-assumed simple, uniform and homogenous reservoir geometry in shale well numerical models represents a problem of non-uniqueness. Another challenge is the fact that relative permeability exponents, rock permeability and even porosity are parameters that are not easily determined by shale core examination. This leaves many reservoir parameters to be determined through history matching, or to be assumed at a value. For instance, relative

---

[1] $C = V_L \frac{p}{p + p_L}$, where C is the volume of adsorbed gas in scf/ton at pressure p, V_L is the Langmuir volume in scf/ft^3, and p_L is the Langmuir pressure in psia.

[2] $R_s = C \frac{0.17525\rho_s}{\varphi S_o}$, where ρ_s is the shale bulk density in g/cc, φ is the formation porosity as a fraction and R_s is the small, immobile oil saturation.

permeability values that are typical of conventional reservoirs are used in this work, while permeability and porosity are derived through history matching.

Even when taking into account all these challenges, the history matching numerical models may still be the best available tool for shale reservoir description and production forecasting to date.

2.3 Analyzing Well Production Using Diagnostic Plots

There exist several plots that are useful for extracting information about a well performance. Plots involving rates and pressures can be useful for determining dominant flow regimes and their duration, well productivity and the comparison of wells through plotting data from multiple wells. For a group of close proximity wells with the same completion type that produce from the same reservoir, and with identical production fluid, differences in production signature can signify local differences in reservoir parameters, differences in completion efficiency, well control differences, interference between wells, etc.

2.3.1 Log-Log Plot

The Log-Log plot is used to identify the dominant flow regimes. Dominant regimes are observed as straight line trends in the plot. Flow regimes that are particularly relatable to fractured unconventional wells are linear flow, bi-linear flow and depletion type flow.

For gas, pseudo-pressure drawdown normalized rate and its log-log derivative with respect to pseudo-time are plotted together versus pseudo-time. In this work, a simplified form of the is used, by substituting pseudo-time with time[3]. The denotations then become

$$\left(\frac{q_g}{p_{pi}-p_{pwf}}\right) vs(t) \quad \text{.....(3.2)}$$

$$\left(-\frac{d(\ln(q/\Delta p_p))}{d(\ln t)}\right) vs(t) \quad \text{.....(3.3)}$$

Where q_g is daily gas rate in Mscf/D, t is time in days, and p_{pi} and p_{pwf} are initial, and current flowing pseudo-pressures in $psia^2/cp$.

[3] Using pseudo-time is not practical for unconventional wells with long-term contribution from the unstimulated reservoir matrix. Calculation of the pseudo-time require information on the average reservoir pressure. Since the reservoir is producing partly in an infinite acting regime for all time periods of practical purposes of well forecasting, the average reservoir pressure becomes difficult to compute analytically, as it requires information on the total reservoir pore volume which can only be achieved when full boundary-dominated flow has been demonstrated.

The definition of gas pseudo-pressure (Al-Husseiny et. Al 1966) is

$$p_p = 2\int_{p_0}^{p} \frac{p}{\mu_g(p)Z(p)}dp \quad \text{.....(3.4)}$$

where p is the current flowing pressure in psia, μ_g is the gas viscosity in cp, Z is the dimensionless real gas compressibility factor and p_0 is a chosen reference pressure in psia. The pseudo-pressure term accounts for several of the pressure dependent gas parameters in the diffusivity equation.

If the normalized rate stabilizes on a constant slope at later times, it indicates boundary-dominated flow. The slope and the intercept can be connected to the diffusivity equation. For a vertical well with a single half-fracture in a closed reservoir with no-flow boundaries and zero contribution from the area beyond the fracture, the constant rate solution to the diffusivity equation during boundary-dominated flow (Wattenbarger, 1998) is:

$$\frac{p_{pi} - p_{pwf}}{q_n} = \frac{\pi}{2}\left(\frac{x_f}{y_e}\right)\frac{t_{Dxfc}}{p_{Dc}}t + \frac{\pi}{6}\left(\frac{y_e}{x_f}\right)\frac{1}{p_{Dc}} + \frac{s}{p_{Dc}} \quad \text{.....(3.5)}$$

Where x_f is fracture half-length and y_e is the distance from fracture to outer boundary, both in feet, and s is a dimensionless, constant skin factor. An illustration of the geometry for the solution is depicted in **Figure 1.**

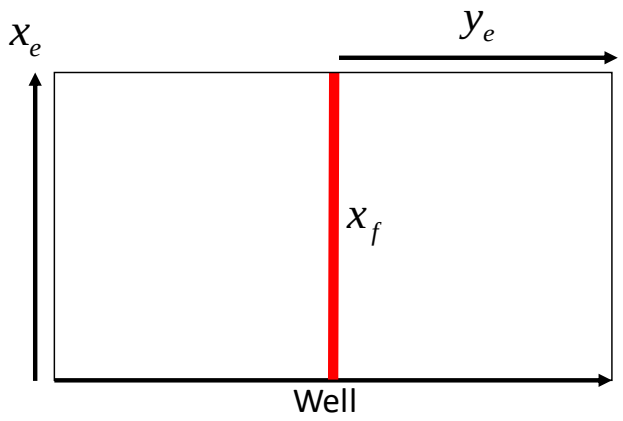

Figure 1: Planar fracture geometry with no-flow boundaries and no contribution from matrix beyond fracture (xe=xf).

The dimensionless time constant is defined as

$$t_{Dxfc} = \frac{0.00633k}{\varphi\mu_i c_{ti} x_f^2} \quad \text{.....(3.6)}$$

and the dimensionless pressure constant is defined as

$$p_{Dc} = \frac{0.703kh}{T} \quad \text{.....(3.7)}$$

Here, k is matrix permeability in mD, h is reservoir thickness in feet, φ is matrix porosity as a fraction, μ_i is initial gas viscosity in cp, c_{ti} is the initial total compressibility in psi^{-1} and T is Temperature in degrees Rankine.

When plotting the data in the form of equation 3.2, the slope during pseudo-steady state becomes

$$m_{PSS} = \frac{2}{\pi}\left(\frac{y_e}{x_f}\right)\frac{p_{Dc}}{t_{Dxfc}} = \frac{hx_f y_e(\varphi c_{ti}\mu_i)}{0.014T} \quad \text{,.....(3.8)}$$

The stabilized slope can be used to calculate reservoir pore volume, provided that values on reservoir temperature, initial fluid viscosity and initial total compressibility are known.

The normalized rate versus time plot is useful for detection of dominant flow regimes when the flowing drawdown pressure is constant, or almost so. In case of more deviation in the operating conditions, and in multi-wall analysis, it is suggested (Anderson et Al., 2010) to substitute time with the superposition function of material balance time. The resulting plot is

$$\left(\frac{q_g}{p_{pi} - p_{pwf}}\right) vs\left(t_{mb}\right) \quad \text{.....(3.9)}$$

$$\left(-\frac{d(\ln(q/\Delta p_p))}{d(\ln t_c)}\right) vs\left(t_{mb}\right), \text{.....(3.10)}$$

where material balance time is defined as

$$t_{mb} = \frac{Q}{q} \quad \text{.....(3.11)}$$

The log-log derivative in equation 3.10 is henceforth known as the slope m_{mb} for convenience.

The material balance time function makes the plot look like the constant rate solution of the diffusivity equation for all combinations of monotonically decreasing rates and flowing pressures. If the well produces in pseudo-steady state, the normalized rate with respect to

material balance time will form a negative unit slope, as is the signature of boundary-dominated flow for the constant rate solution.

For a planar fracture reservoir geometry and with infinite conductivity fractures, early linear flow is expected. This can be observed as a negative half slope, and as a constant value of 0.5 of the derivative m_{mb}. This early flow is dominated by the one-dimensional linear flow from the matrix blocks $x_f y_e$ to the fractures. If included, the outer, unstimulated reservoir ($x_e > x_f$) is likely to provide a negligible contribution to the early flow.

In the dimensionless constant rate flow equation, the skin is a constant. Subsequently, the derivative of the normalized rate does thus not contain skin. Therefore, the slope of the derivative should be used primarily for detecting dominant flow regimes, as the normalized rate slope may be polluted due to skin.

The plot is useful for comparing production signatures of neighboring wells, if rates and pressures are available. A Log-Log plot with data from multiple wells can be used to identify similar well signatures, specifically by identifying flow regimes and their duration.

If linear flow is detected in the Log-Log plot, it allows for analysis using the Linear flow specialized plot.

2.3.2 Linear Flow Specialized Plot

The Linear Flow Specialized plot or LIA (Linear Infinite Acting) plot, is used for determining duration of the linear flow regime, detecting constant skin and estimate reservoir parameters. Linear flow is represented as a straight line in the plot. Departure from linear flow is observed as a departure from the linear trend.

In many unconventional reservoirs, linear flow is often seen to be the dominant flow regime for extended periods of production, often months or even years. Due to the ultra-low permeability, the flowing pressure drops relatively quickly and stabilizes, which allows for extracting parameters from the specialized plot with the assumption of a constant drawdown.

However, in cases where wells demonstrate a limited period of early linear flow, varying pressures must be accounted for as the flowing pressure might not yet be stable. The function of linear flow superposition (Fetkovich and Vienot, 1984) is applied to account for varying rates and pressures.

The linear flow plot used in this work is the following;

$$\left(\frac{p_{pi}-p_{pwf}}{q_g}\right) vs\left(f_{cp}t_{LS}\right) \quad \text{.....(3.12)}$$

Where the linear superposition time t_{LS} is

$$t_{LS}=\sum_{j-1}^{n}\frac{(q_j-q_{j-1})}{q_n}\sqrt{t_n-t_{j-1}} \quad \text{.....(3.13)}$$

The superposition function, as previously mentioned, accounts for data with varying rates and pressures. f_{cp} is the Ibrahim and Wattenbarger (2006) empirical correction factor for pressure dependent gas parameters in the dimensionless time constant t_{Dxfc} (equation 3.6). It is defined as

$$f_{cp}=1-0.0852D_D-0.0857D_D^2 \quad \text{.....(3.14)}$$

Where the dimensionless drawdown is defined as

$$D_D=\frac{p_{pi}-p_{pwf}}{p_{pi}} \quad \text{.....(3.15)}$$

The correction factor is shown (Nystad, 2015) to be applicable for varying rates and pressures.

Like in the Log-Log plot section, a closed planar half-fracture reservoir is assumed. Then, the constant rate solution to the diffusivity equation with infinite acting linear flow (Wattenbarger 1998) is:

$$\frac{p_{pi}-p_{pwf}}{q_n}=\frac{s}{p_{Dc}}+f_{cp}\frac{\sqrt{\pi t_{Dxfc}}}{p_{Dc}}t_{LS} \quad \text{.....(3.16)}$$

This means that when data is plotted and forming a straight line, the slope m of the straight line is

$$m_{LF}=\frac{\sqrt{\pi t_{Dxfc}}}{p_{Dc}}=\frac{0.2006T}{h\sqrt{\varphi\mu_i c_{ti}}}\frac{1}{x_f\sqrt{k}} \quad \text{.....(3.17)}$$

Again, this is the solution for a single half-fracture in a bounded reservoir. Scaling up to well data, the slope is multiplied by the inverse of the number of fracture units. Adsorption and pressure dependent rock and fracture properties can be included, but is not discussed further in this work.

When plotting real well data in the two plots, the Log-Log plot and the specialized linear plot, it is very challenging to extract information on single parameters. To extract information on particular parameters with the analytical solutions, it requires detailed information on the majority of the parameters in equations 3.8 and 3.17. This, again, is not easily done for shale. It is the authors opinion that it would be very speculative in nature to determine specific values for real well reservoir parameters based on the slope values in the two plots. Using the lump parameters as a guide for the well performance and productivity is a more conservative approach. Equation 3.8 can be used to estimate the reservoir pore volume and equation 3.17 can indicate the product of the square-root of permeability, the square-root of porosity and fracture-half length, as the remaining parameters are not too difficult to determine in a dry gas reservoir.

Further, in the Log-Log plot when reviewing long-term production, it is possible that in real well cases the outer reservoir contributes considerably. A contributing outer reservoir would change the analytical solution and the relationship in equation 3.8 could not be used.

In this work, the plots are rather used as a tool for group assessment, to compare relative well performances and to observe a unique group trend among wells using rates and pressures. This can be that the wells share the same flow regimes and durations, have similar values of skin and share an overall common signature. Even for a group of similarly-completed gas wells within the same area, reservoir parameters like thickness, permeability and porosity can differ significantly. By identifying a unique group behavior, it gives confidence in that the wells indeed are very similar, and are likely to perform similarly in the future.

.

3. The Log-Log Derivative of Pseudo-Pressure Normalized Rate with Respect to Material Balance Time (m_{mb})

When flowing pressures are not constant, rates should be substituted with pseudo-pressure drawdown normalized rate. When analyzing multiple wells in a plot, it is, as previously stated, convenient to utilize the material balance time function to minimize the effect of differing operating conditions. The pseudo-pressure drawdown normalized rate with respect to material balance time effectively accounts for varying pressures and minimizes differences due to differing operating conditions amongst a group of wells.

Three cases are simulated to demonstrate how the derivative m_{mb} behaves. A numerical model is constructed with a planar fracture geometry, with evenly spaced infinite conductivity fractures in a reservoir with homogenous and constant rock parameters. A sketch of the numerical model geometry utilized to produce these rates is illustrated in **Figure 2**. The dotted lines represent the gridding, and it can be seen that finer gridding is used closer to the fracture. **Figure 3** shows the normalized decline gas rates versus material balance time and the slope value m_{mb} for three different cases, whilst **Figure 4** shows the flowing pressure profile and gas rates versus time on a semi-log plot.

The three cases are identical with the exception of matrix area beyond the planar fracture tips. The flowing pressure profiles are identical and monotonically decreasing until stabilizing at a constant flowing pressure.

In the Log-Log plot in **Figure 3**, all cases demonstrate an early straight line trend with a slope value of negative 0.5, indicating linear flow. This is also seen by the value of 0.5 of the derivative. At a relatively early stage, the slope value m_{mb} for all cases increases, indicating boundary effects. The case with no matrix contribution beyond the fracture tips gradually increases its slope value towards 1. At approximately 1200 days, the reservoir pressure stabilizes, and the case with xe/xf=1 produces in full depletion, denoted by the negative unit slope and the constant derivative value of 1. The two cases with matrix beyond fracture tips experience a late dominant transient flow, as seen by the reduction in the derivative value. Later, both cases experience a second round of boundary effects. None of the two cases are even close to converge (the model is run for 60 years). After 30 years of production, the two latter cases produce 180% and 196% compared to the case with no unstimulated matrix contribution.

The cases are constructed to illustrate three points; 1) For a case with planar, infinite conductivity fractures with monotonically decreasing rates and bottomhole pressures, the derivative m_{mb} will always maintain a value between 0.5 (early linear flow) and 1 (full depletion). 2) If well control stays stable, then a reduction in the value of the derivative indicates transient flow dominance. An increase in value indicates boundary-flow dominance. Ultimately, the value of the derivative will reach a value of 1, provided that outer boundaries exist. 3) In a longer time-frame and still with ultra-low permeability (the value of permeability in the examples is 100 nD), the contribution from the surrounding matrix can be substantial and is denoted by a late decrease in the derivative m_{mb}. If such a behavior is observed for real well data after the first boundary-dominated flow period, it may signify a long well-life with a steady long-term production from the unstimulated reservoir.

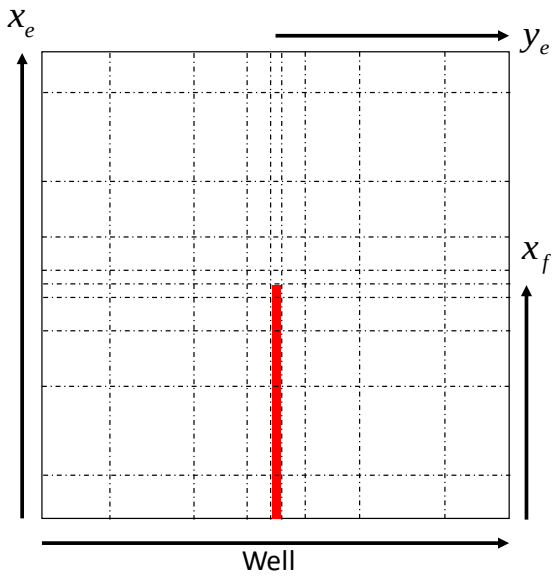

Figure 2: Sketch of the Planar Fracture Model with a contributing matrix beyond the fracture tip.

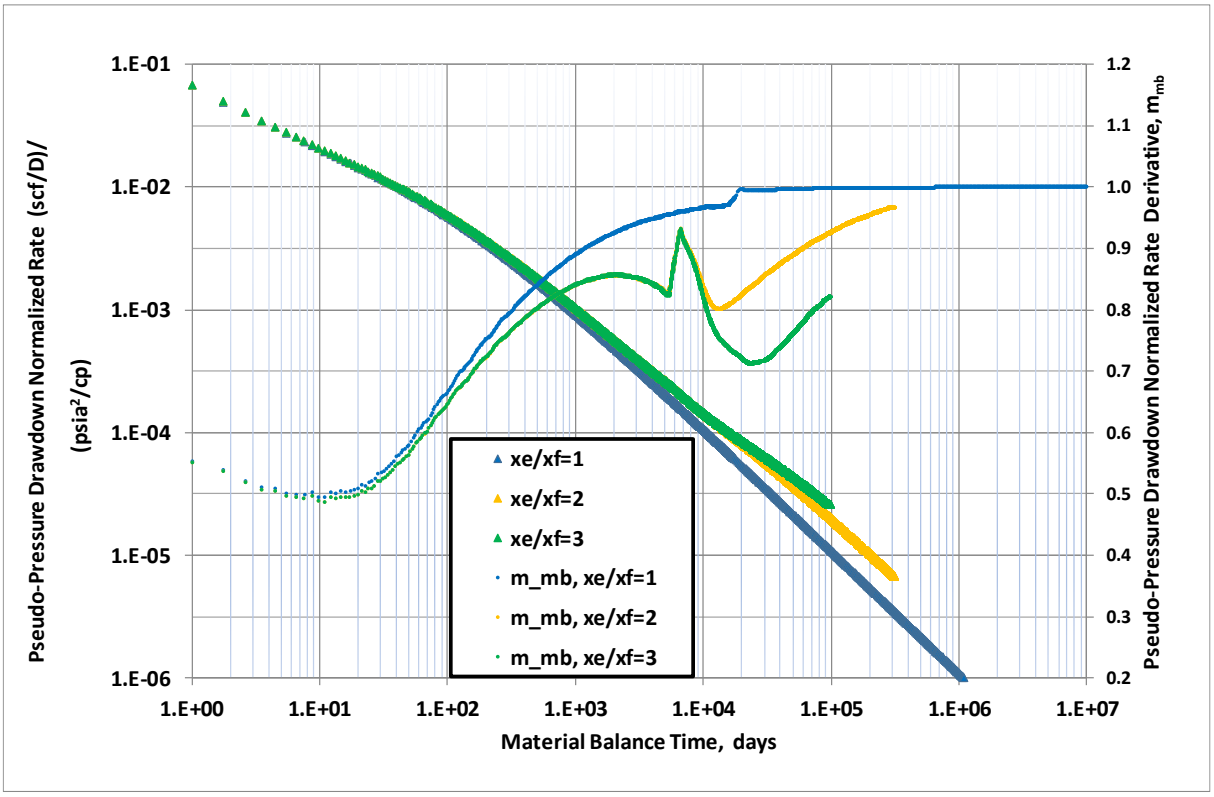

Figure 3: Planar fracture simulated cases with differing area beyond fracture tip. The case with zero unstimulated area shows only boundary-dominated flow after the early LIA flow, which can be seen as the ever-increasing value of the derivative m_{mb}. When bottomhole pressure stabilizes, the well produces in full depletion. Increased unstimulated area yields a greater later transient flow contribution, denoted by the reduced value of the derivative m_{mb}.

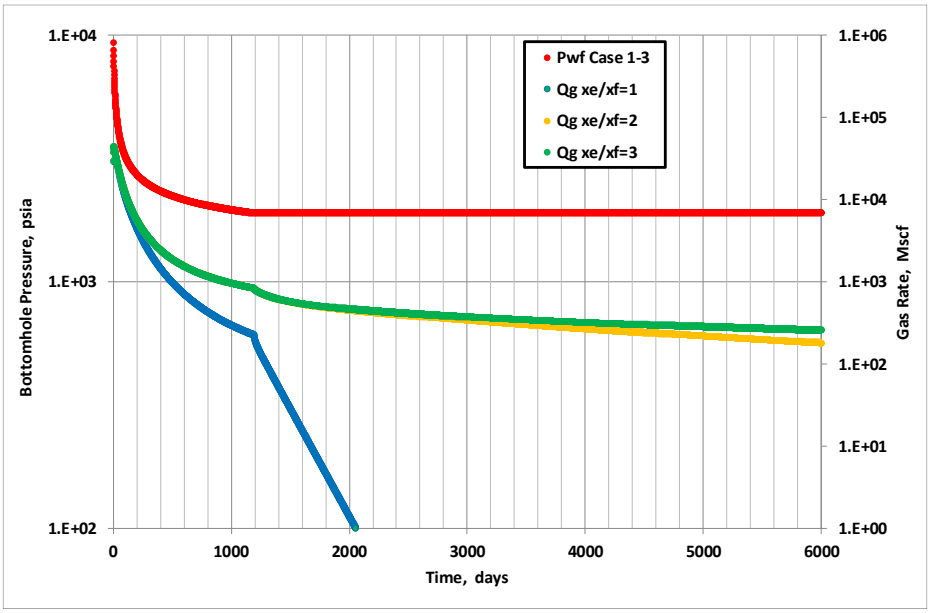

Figure 4: Rates and pressure profiles for cases with differing area beyond fracture tip.

The Arps nominal decline evaluates rate loss with respect to time. The derivative m_{mb} evaluates pseudo-pressure drawdown normalized rate loss with respect to material balance time. The difference in the two can be said to be that

1) the derivative m_{mb} applies to cases with varying flowing pressures.

2) in multi-well plots, the substitution of time with material balance time balances out differences due to differing well controls.

3) for a planar fracture reservoir with infinite conductivity fractures and monotonically decreasing rates, the derivative m_{mb} will always have a value between 0.5 and 1.

4. Method Overview

A case can be made that if a unique group trend is observed amongst a group of wells into the later transient period which is dominated by unstimulated matrix production, then a forecast with a history matched numerical model for a representative well in the group could be used as a "guide" for how the remaining wells will produce in the future. Such a procedure could capture more of the transient matrix flow contribution, while still being constrained by the representative wells' model.

In this work, a specific workflow for forecasting a group wells is presented, and results for a number of real-well cases are provided. In short, the workflow is as follows;

- Gather rate and pressure data for a number of wells in an area. All wells should be producing from the same formation, and have a similar-type completion (i.e. horizontal well with evenly spaced perforation clusters along the wellbore). The wells are all assumed to produce the same dry gas, i.e. the specific gravity is assumed identical. Reservoir temperature (or well depth) is assumed identical for all wells.
- Identify if a unique group behavior exists among the wells, by reviewing multi-well plots, specifically the Log-Log plot and the LIA specialized plot. Essentially, the procedure of defining a group behavior is put in place to identify wells that are more likely to demonstrate a similar future signature.
- Select one representative well from the group that be history matched and forecasted with a numerical model on constant pressure drawdown (equal to the pressure of the last days of history, provided that a constant pressure drawdown production is already the trend). The forecasted rates for the representative well provides a full-life well signature to be put back into the log-log plot.
- The remaining wells that demonstrate a unique group signature, are forecasted by, specifically, extending the trend of the derivative m_{mb} to the other wells. Several forecasts with different trajectories of the derivative m_{mb} are provided, but tied to the representative wells' end points.

The procedure is essentially a use of the guidelines for grouping wells by Collins et Al. (2015), whilst, like Pratikno and Reese (2014), continuously evaluating the well production derivative and ultimately following the suggestion by Whitson et Al. (2016) that a history matched model be serving as a supporting tool for calibrating some DCA method. The difference in this work compared to Collins' guidelines, is the removal of the semi-log normalized rate versus

cumulative production plot, and the inclusion of the log-log derivative of normalized rate with respect to material balance time, m_{mb}. Further, instead of evaluating the derivative of rate with respect to time (the nominal decline), and assuming constant drawdown, this work evaluates the normalized rate with respect to material balance time, allowing for varying pressures and differing well controls. Instead of using the Arps equation for forecasting, the derivative m_{mb} is extended, guided by a similar producing wells' complete life signature, to produce a number of forecasts.

The next subchapters provide a walkthrough of the procedure.

4.1 Identify a Unique Group Signature and Select a Representative Well

The objective of grouping wells based on some criteria is to increase the likelihood that the wells will produce similarly in the future.

Collins and Ilk (2015) suggest that the wells in a group should satisfy the following conditions:

- Exhibit identical flow regimes and unique characteristics behavior, which means that a characteristic solution exists and could be applicable for this group of wells
- Produce in a close proximity, have similar fluid properties and similar type completions

Firstly, the grouped wells should all produce in the same area and from the same formation. This criterion narrows the value ranges of a number of reservoir parameters that determines production. Matrix porosity, matrix permeability and water saturation are parameters of this nature. Gas specific gravity and reservoir Temperature are assumed identical for close proximity wells.

Secondly, the completion procedure for all wells should be similar. This criterion limits the chances of the wells having differing geometry downhole and thus flow regimes and their duration.

Thirdly, the wells that fit with the aforementioned criteria, are analyzed using diagnostic plots. The key objective is to identify a characteristic group behavior, which, in turn, increase the likelihood for the wells to behave similarly in the future.
The analysis includes a) to observe if the wells demonstrate identical flow signatures and b) to observe if wells stay in the different flow regimes for similarly long periods.

The following plots, in addition to production and pressure history plots, are utilized for group assessment and for demonstrating a unique group behavior:

- Log-log pseudo-pressure drawdown normalized rate versus material balance time for flow regime identification and comparing well performance.
- Cartesian rate-normalized pseudo-pressure drawdown versus linear flow superposition time function for identifying linear flow duration, apparent skin and relative well performance.
- Log-log - $\frac{d(\ln(\frac{q}{\Delta p_p}))}{d(\ln(t_{mb}))}$ vs material balance time for production analysis and forecasting.

Daily production rates and tubinghead pressures should be acquired to produce the aforementioned plots. Bottomhole pressures are calculated from recorded casing pressures and, when installed, tubing pressures, using an appropriate empirical correlation for dry gas. Empirical correlations are also used to calculate pseudo-critical values of pressure and temperature of the gas, which again are used to calculate the viscosity and real gas factor Z, allowing for the calculation of pseudo-pressures.

For the calculation of the derivative m_{mb}, the Bourdet Algorithm (1989) is utilized because of its ability to smoothen the signal. It is important that the smoothing factor used is constrained, so that the overall signature is not changed.

A well that demonstrates all characteristic group traits in the plots and that is considered a representative well, is selected for numerical modeling and history matching. It is preferred that this representative well has a long production history, as this narrows the reservoir parameter ranges for which a good history match may be achieved.

4.2 Perform History Match and Produce a Forecast for the Selected Well

When a well is selected and deemed a representative well for the group, a numerical model is subsequently constructed and history matched to historical data.

Apart from rate and pressure data, the numerical model requires data on well completion and reservoir to construct a model, which must be acquired from the well operator.

For a planar fracture geometry, it is assumed that a single fracture, perpendicular to the wellbore, exists at each perforation cluster. A set of default values for the properties of the fracture conductivity are applied (Golan and Whitson, 1987). As a default, fractures are

assumed identical and evenly spaced along the wellbore. The volume of the reservoir is determined by obtaining data on reservoir thickness, wellbore length and distance to neighboring wells. Some reservoir properties may be modeled as pressure sensitive, like fracture permeability or rock compressibility.

The model is then run and history matched to the calculated bottomhole pressures (from historical tubing pressures). A set of unknown variables are varied to match the model to historical data. Matrix permeability, fracture half-length, matrix porosity and water saturations are typical parameters matched in this procedure.

If the history match follows the calculated bottomhole pressures closely throughout the history, and the matched history itself covers a long time-span, it gives confidence in that the model is an adequate representation of the reservoir downhole. If no good match can be achieved, one may proceed to match the well with a different model geometry, or perform a more thorough diagnostic.

When a history matched model is decided upon, a forecast is produced by running the model for an extended period of time; e.g. 30 years. A standard forecast procedure would be to forecast the well on constant bottomhole pressure, using the last historical value.

The generated forecast rates provide a full-life well signature, and this signature is plotted in the aforementioned Log-Log plot together with the similarly performing wells to serve as a forecasting tool for the remaining wells.

4.3 Perform Forecasts for the Remaining Wells in the Group

The history matched model data are plotted in the Log-Log plot, providing a complete well-life signature. The derivative m_{mb} in the Log-Log plot is examined and plotted with the derivatives of the remaining wells. In **Figure 5**, a similar performing well is compared to a full life-signature well in the Log-Log plot. As can be seen, the two wells demonstrate a similar trend. The sudden spike of the derivative m_{mb} reflects that the monotonically decreasing bottomhole pressure is stabilized on a constant value.

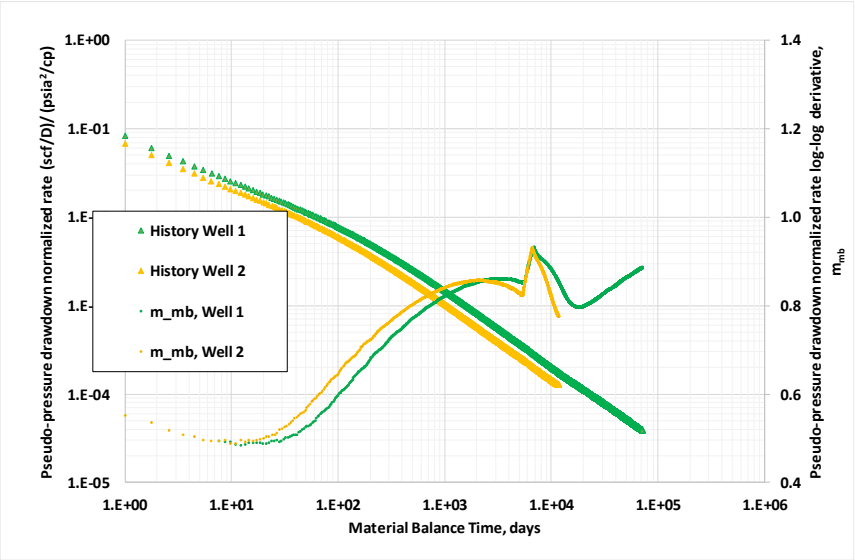

Figure 5:Synthetic Wells Example -- Two similar behaving wells, one of which has a complete life signature.

The basic assumption for the primary forecast is that the well at hand will behave similarly to the modeled well in the future, as it has done in the past. In the forecast, the curvature of the derivative m_{mb} of the modeled well is extended to the other well, but shifted on the "y-axis", so that it continues the trend from the last historical value. The newly produced forecast of the derivative m_{mb} is then used to calculate rate, time and cumulative production for each material balance time step. **Figure 6** shows how the trend of the full-life well derivative is applied to the other well.

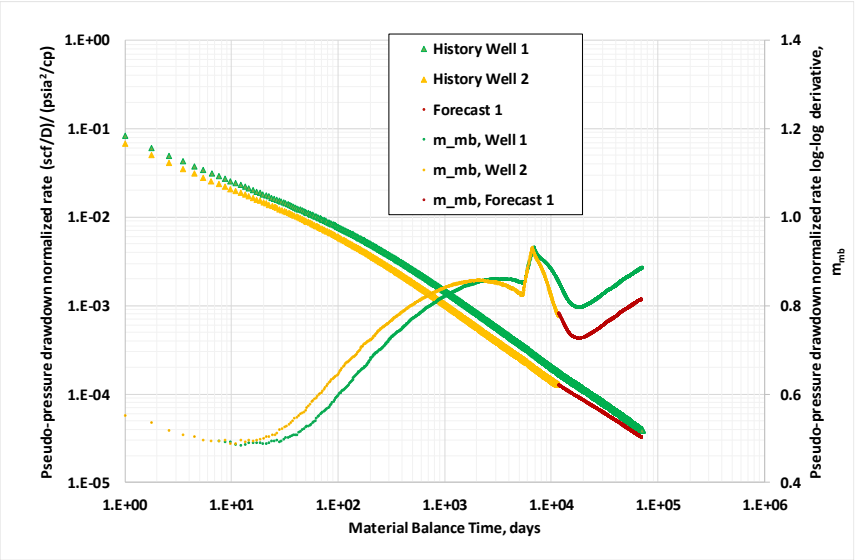

Figure 6: Synthetic wells example -- Two similar behaving wells, one of which is forecasted by the other wells' complete life signature. The derivative m_{mb} of the full-life signature is applied to the other wells' end point value.

Two additional forecasts are produced, both of which have starting and ending values identical to that of the primary forecast. The derivative of forecast 2 increases rapidly, providing a slightly more pessimistic forecast, while forecast 3 maintains lower values of m_{mb} before making a sudden increase towards the end value. All three forecasted m_{mb}-slopes are provided in **Figure 7.**

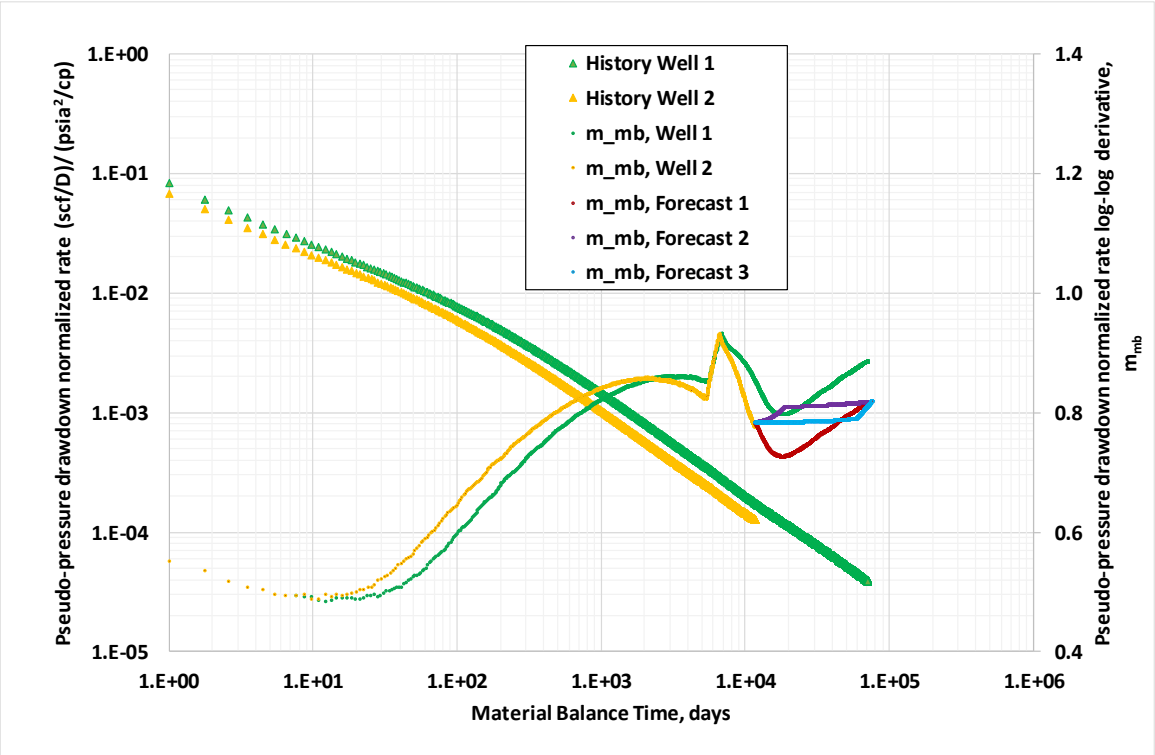

Figure 7: Synthetic wells example -- Three different trajectories for the derivative m_{mb}, sharing start and end point values.

Forecast 2 and 3 maintain values for m_{mb} within the range of the starting and ending values. Forecast 2 derivative trajectory increases faster, yielding a more pessimistic forecast.

Utilizing the produced forecast values of the derivative m_{mb}, rate, time and cumulative production are calculated. **Figure 8** shows a plot of cumulative gas produced versus time derived from the three forecast-trajectories.

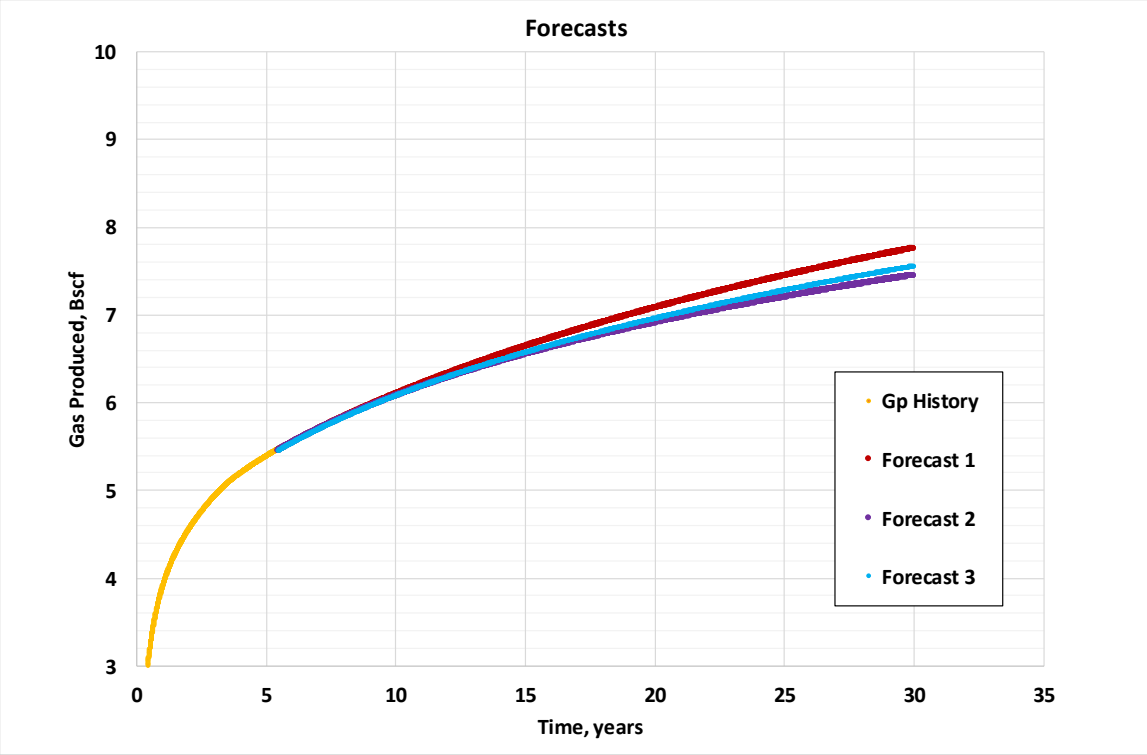

Figure 8: Synthetic wells example -- Cumulative gas produced versus time.

Table 1 summarizes the forecast values for this particular case. For comparison purposes, a full-life model of the well at hand is provided. The numerical model has a planar fracture geometry with a fixed reservoir width. In this particular case, the primary forecast is yielding the same ultimate recovery as the full life numerical model. EUR is either constrained by time (30 years) or minimum economic rate (50 Mscf/D).

Table 1: Synthetic wells Example -- Forecast values summary.

Forecasts Synthetic wells example		
Forecast	**Production Time**	**Gp**
[#]	**[years]**	**[bscf]**
1	30	7.8
2	30	7.4
3	30	7.6
Full-life model	30	7.8

The basic assumption of the procedure is that if a unique behavior is observed amongst a group of wells, then the behavior will continue to be unique for all wells in the future. A second assumption is that the produced history matched model is an acceptable (good enough) representation of the true reservoir downhole for that well. With these assumptions, it can be said that the forecasts conducted with the proposed method is a decline curve procedure that is rooted in the physics that govern flow through porous media.

5. Real Wells Forecasting and Results

The procedure is performed for a group of five real dry gas shale wells. The five wells are producing in close proximity, and from the same reservoir, namely the Haynesville formation.

5.1 Real Wells: Identifying a Unique Group Signature and Selecting a Representative Well

Data on daily gas rates, water rates and tubinghead pressures for five standalone horizontal gas wells is gathered. The gas specific gravity and reservoir depth for one well is acquired and assumed identical for the remaining wells. Their history span from less than three years to over five years of production. **Figure 9** shows the rates versus time. The wells have high early daily rates followed by a rapid decline and steady long term production, which is typical behavior for fractured shale wells.

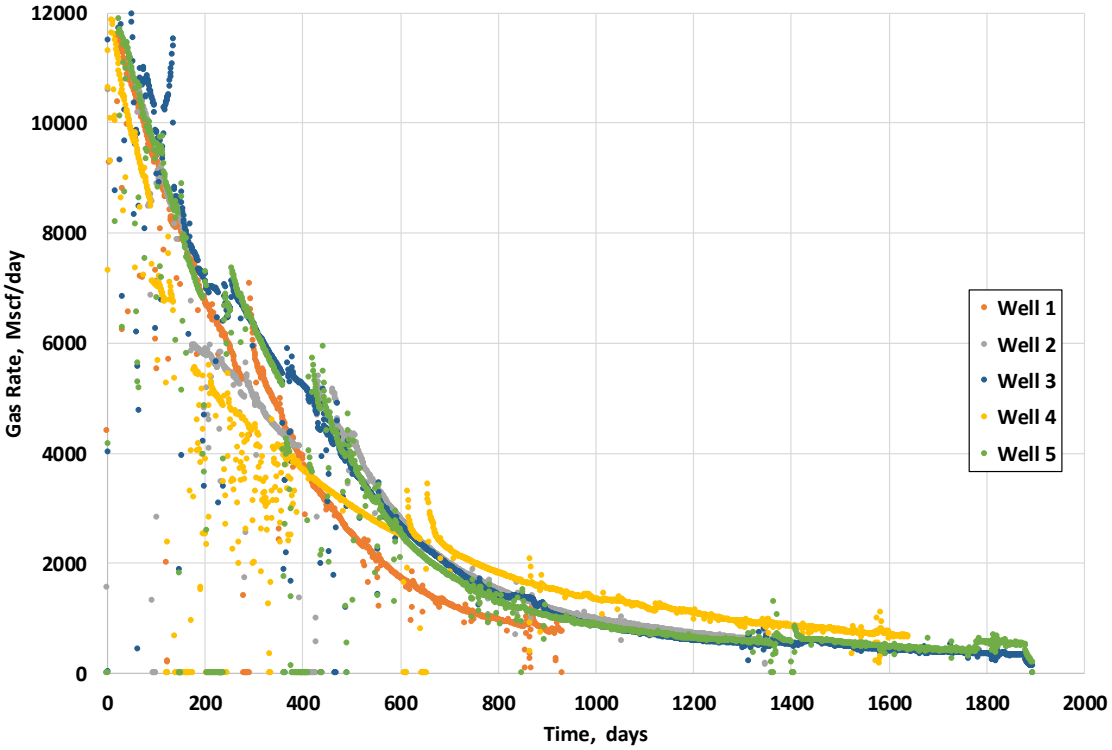

Figure 9: Gas rate versus time for all wells.

Bottomhole pressures are calculated from the provided tubinghead pressures, rates and reservoir depth, by using the Gray Correlation which calculates the hydrostatic pressure column and pressure loss due to friction in the vertical wellbore. A tubing diameter value is assumed for calculation of the friction pressure loss.

After around three years, all wells stabilize at a constant bottomhole pressure at approximately 2000 psia.

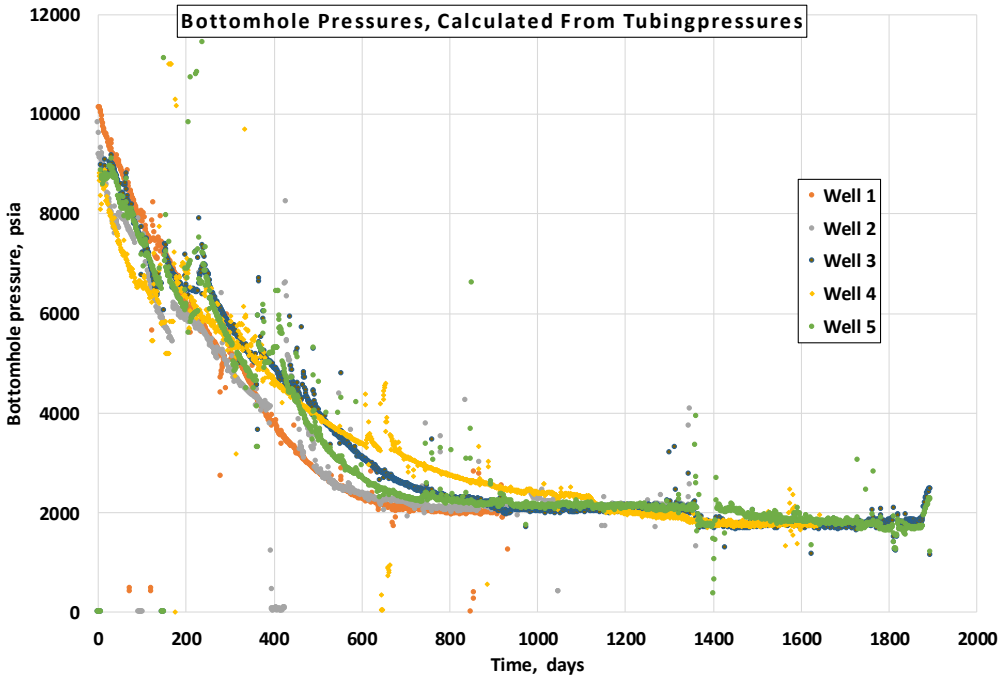

Figure 10: Bottomhole flowing pressure versus time for all wells. All wells stabilize at around 2000 psia after 2-4 years.

The monthly average water-gas ratios are presented in **Figure 11**. All wells demonstrate long-term ratios of under 1.5 percent. Well 4 has a distinct greater early water production but later stabilizes on 1.1 percent.

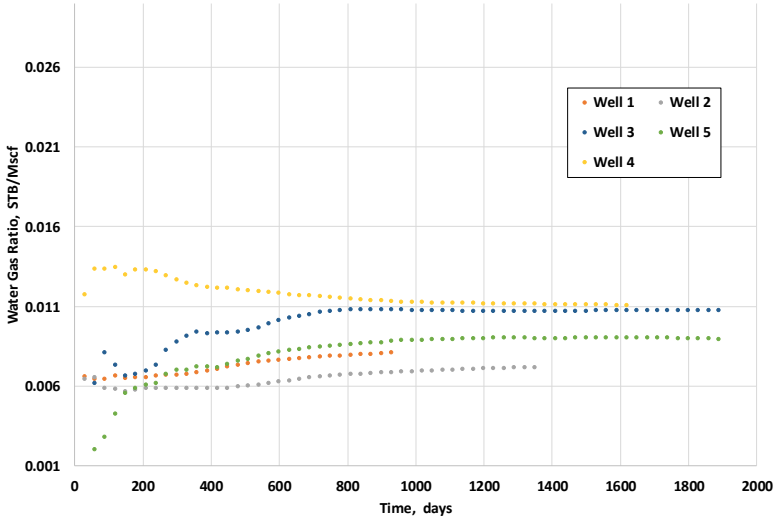

Figure 11: Water-gas ratio for all wells.

Critical gas pressure and temperature are calculated with the Sutton (1985) correlation to calculate the real gas factor Z. The viscosity is subsequently calculated with the Lee et Al. (1966) correlation, providing pseudo-pressure values. The Log-Log plot for pseudo-pressure drawdown normalized rate versus material balance time for all wells is depicted in **Figure 12**.

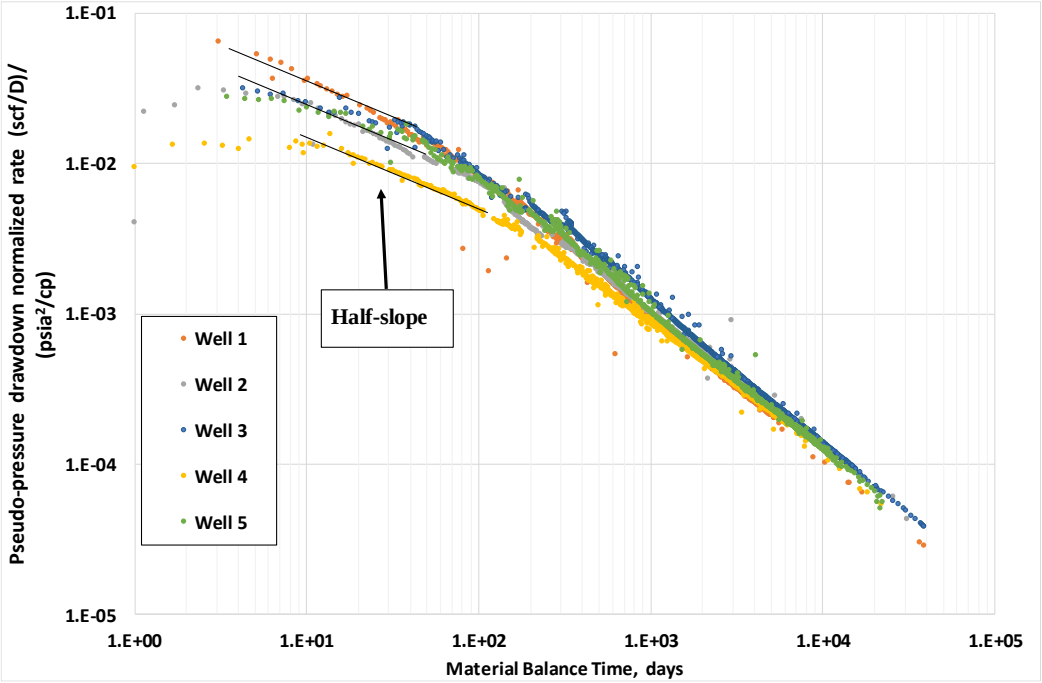

Figure 12: Pseudo-pressure drawdown normalized rate versus material balance time for all wells. All wells demonstrate an early half-slope, indicating linear flow. Case 4 deviates slightly from the later trend, demonstrating a shallower slope.

All wells exhibit the characteristic negative half-slope, indicating early linear flow. At a relatively early stage for all wells, there is observed a distinct slope value increase, indicating boundary effects. For the rest of the history, all well slopes exhibit a more or less stabilized slope value, none of which are unit slope. Well 4 has a notable shallower slope than the rest of the group, possibly indicating that a greater percentage of its total production comes from transient flow periods. It looks to be stabilizing together with the other wells at later times, possibly indicating that the reduced early production is due to a less effective well completion and not due to significant differences in OGIP.

The derivatives m_{mb} for all wells are presented in **Figure 13**. Although scattered, the trend among the wells is an increasing value towards and beyond 1, before a decrease and stabilization somewhere between 0.75 and 1. The reason for the derivative surpassing 1 is due to sudden increase in rates, i.e. production following a shut-in. A boundary dominated regime is characterized by ever-increasing values towards 1. The decrease in the value of the derivative after the spike, followed by a stabilized period, could signify a dominant infinite acting regime. This is possibly due to a dominant flow from the unstimulated matrix, after the stimulated reservoir volume is effectively drained.

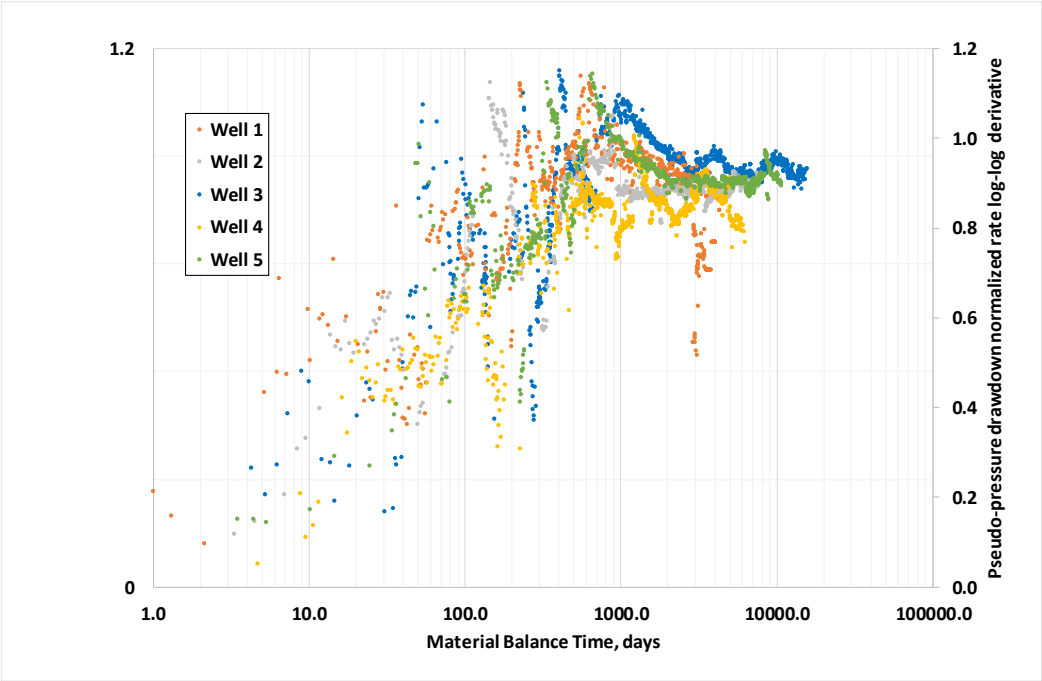

Figure 13: Derivative slope m_{mb} for all wells. All wells show an early increase, indicating BD flow, before reaching a top and a slight decline, indicating a late infinite acting flow contribution.

The Wattenbarger corrected linear flow specialized plot for variable rates and pressures is presented in **Figure 14**. The plot suggests that well 4 is experiencing an early positive skin when compared to the rest of the group, as it is shifted upwards. Wells 2,3 and 5 also do seem to have a slight positive skin. The well slopes are not very different from each other, though well 4 looks to have the steepest slope. The similar slope values suggest that the wells have very similar performances. The apparent very short period of infinite acting linear flow is a common group trait. Without any more knowledge on the wells, it is difficult to identify what could be the reason for this early departure. A very good completion efficiency could be the reason, another possibility is that some reservoir parameters are pressure dependent, causing the upward deviation and effectively masking the linear flow period.

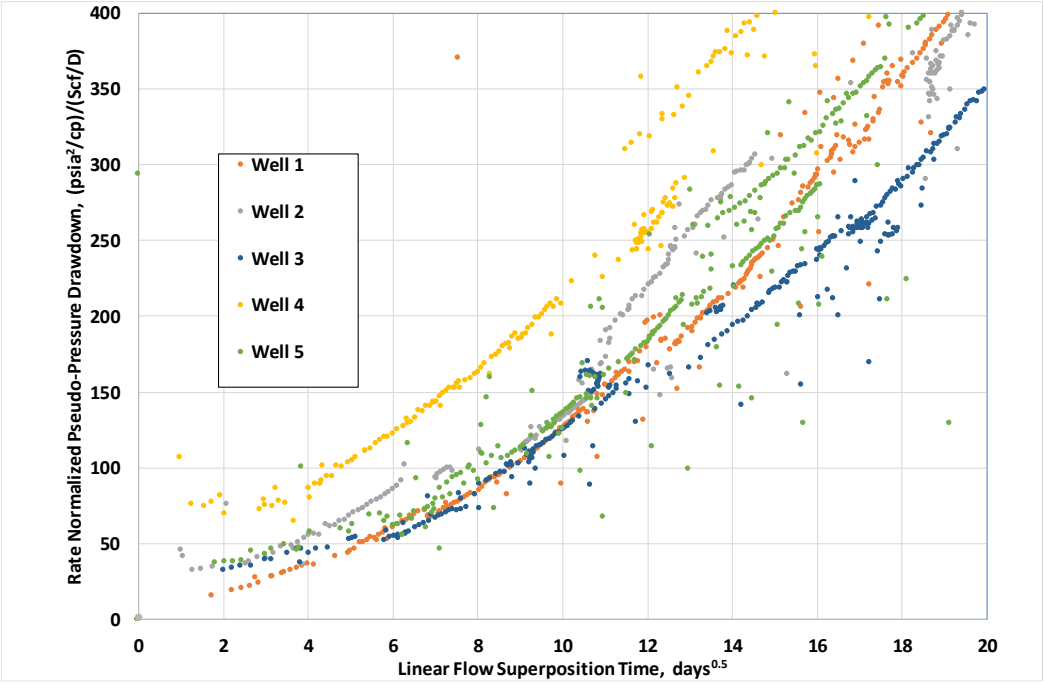

Figure 14: Linear Flow Specialized plot all wells. Slope of well 4 is shifted up, indicating a positive skin. All wells demonstrate an apparent very short linear flow regime period.

5.2 Real Wells: Perform History Match and Produce a Forecast for the Selected Well

Well 5 is selected for numerical modeling and history matching. It demonstrates all characteristics of the group signature and has a long production history.

Completion and reservoir data for well 5 is acquired from the operator. **Table 2** presents the well model parameters.

Table 2: Representative well acquired reservoir and completion data.

Variable	Value	Unit
Horizontal Well Length	4330	ft
Well Spacing	80	acre
Number of Perf. Clusters	56	
Tubing inner diameter	1.995	in
Tubing Set Depth	10335	ft
Casing inner diameter	4.67	in
TVD	11920	ft
Reservoir thickness	170	ft

Initial Reservoir Pressure	10490	psia
Reservoir temperature	320	°F
Rock density	2.72	g/cc
Langmuir Volume	60	Scf/ton
Langmuir Pressure	1000	psia

A planar fracture model is constructed with the acquired data, where homogenous, equally long fractures are assumed at each perforation cluster. Fracture properties are assumed at some default values (Golan and Whitson, 1987), yielding infinite fracture conductivity. Relative permeability exponents and formation compressibility are assumed at some default values. However, water production is matched by altering the water saturations and the water relative permeability exponent. Reasonable water cut matches were achieved, but without trying to capture a detailed trend. The reservoir simulator calculates the relative permeability curves analytically, using the equations of the Brooks-Corey power law (1964). Relative permeability data is presented below.

Table 3: Relative permeability data for numerical history matched model.

Relative Permeability data			
$\mathbf{k_{rw}}$	1	$\mathbf{n_g}$	3
$\mathbf{k_{rg}}$	1	$\mathbf{n_{og}}$	3
$\mathbf{k_{ro}}$	1	$\mathbf{S_{wc}}$	0.01
$\mathbf{n_w}$	1.7	$\mathbf{S_{orw}}$	0.0015
$\mathbf{n_{ow}}$	3	$\mathbf{S_{org}}$	0.0015
		$\mathbf{S_{gc}}$	0.1

The model is history matched to historical data until a set of unknown reservoir parameters are decided upon. It was found that for this well, a good history match could only be obtained with a pressure dependent fracture permeability. The apparent very early departure form linear flow is therefore explained by pressure dependent fractures. A relatively large matrix permeability was obtained, at 520 nD. For this model, the matrix permeability would also comprise any natural fracture network within the matrix. The values for the derived history matched reservoir parameters are presented below

Table 4: Derived reservoir parameters from history matching

Variable	Value	Unit
Formation permeability	520	Nd
Formation porosity	4.6	Percent
Fracture half-length	390	ft
Initial Water Saturation	0.23	-
Connate Water saturation	0.03	-
Pressure dependent fracture permeability exponent	0.62	

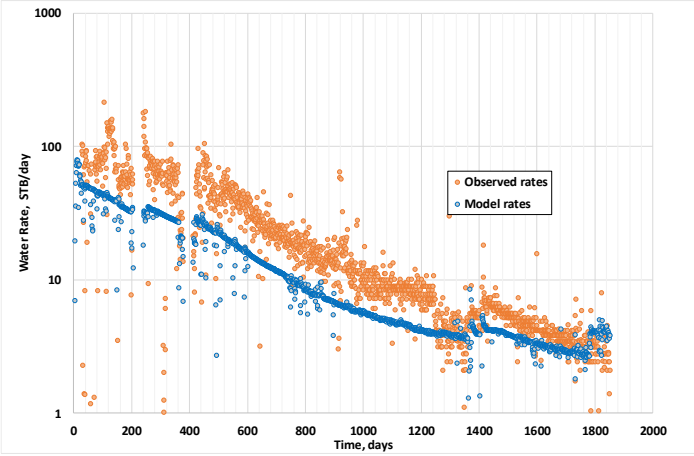

Figure 15: Water Rate match.

Depicted in **Figure 16** are the bottomhole pressures for the history matched model compared to the historical, calculated bottomhole pressures. As can be viewed from the plot, the model follows the historical pressures well for the entire history of five years, with some small discrepancies.

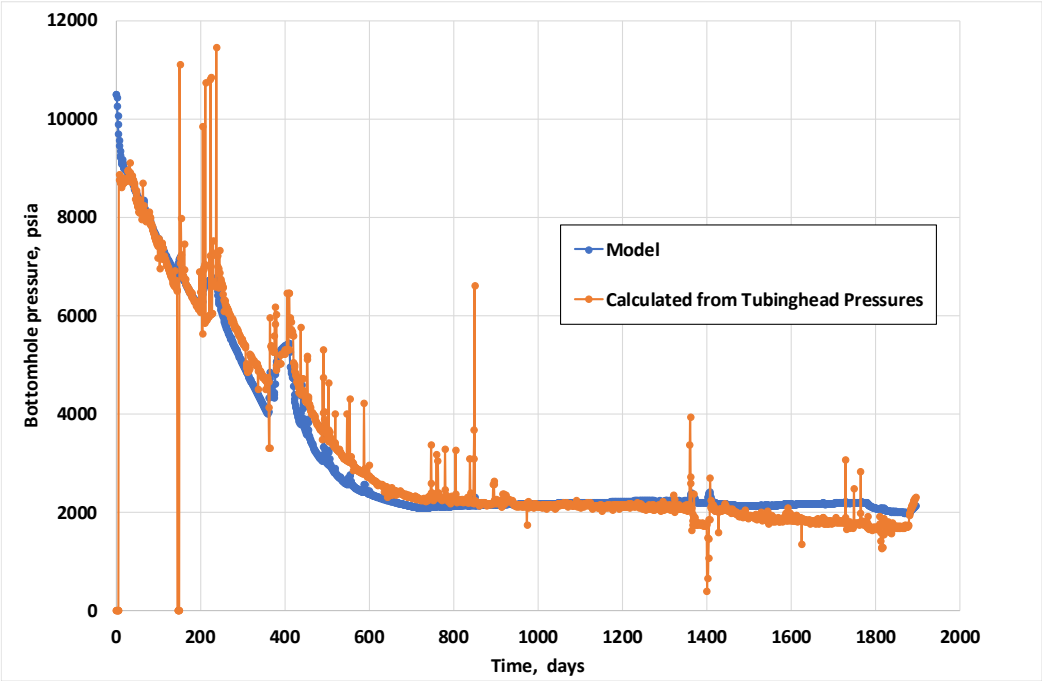

Figure 16: Representative well - history matched models' bottomhole pressure compared to historical bottomhole pressures calculated from tubinghead pressures.

In the figure below, the analytical slope constructed with parameters derived from the history match, is plotted together with historical data in the linear specialized plot. The slope value is roughly similar to the early historical trend. The upward deviation is assumed to be caused by deterioration of the fractures.

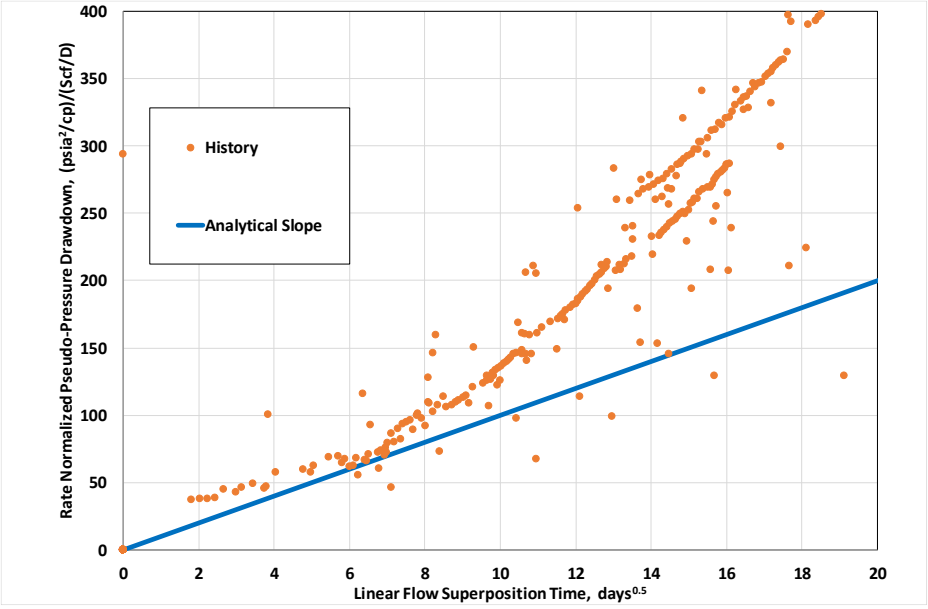

Figure 17: LIA plot with historical values and analytical slope with parameters derived from history match.

A forecast is produced on constant bottomhole pressure from the last historical trend. Values for pseudo-pressure normalized rate and its derivative with respect to material balance time are

obtained and plotted in the Log-Log plot. Wells 1-4 are subsequently forecasted with the modeled wells' signature and adjusted on the y-axis to fit the historical trend.

5.3 Real Wells: Perform Forecasts for the Remaining Wells in the Group

5.3.1 Well 1

The history of well 1 is shown to be very similar to the modeled well (Well 5) in all parts. The derivative m_{mb} is evaluated for each time step with the Bourdet Algorithm. The well 1 derivative value follows the trend of that of the modeled well, but demonstrates slightly greater values per material balance time step in the apparent second transient period. The base forecast extends the trend of the modeled well to well 1, but shifted slightly down on the y-axis in order to continue from the historical values. **Figure 19** provides the trajectories for the derivatives m_{mb} for forecast 2 and 3. **Figure 20** and **Table 5** present the cumulative production in graph and table format, respectively. Included in the table are the actual history matched numerical model forecast values for each well, for comparison purposes.

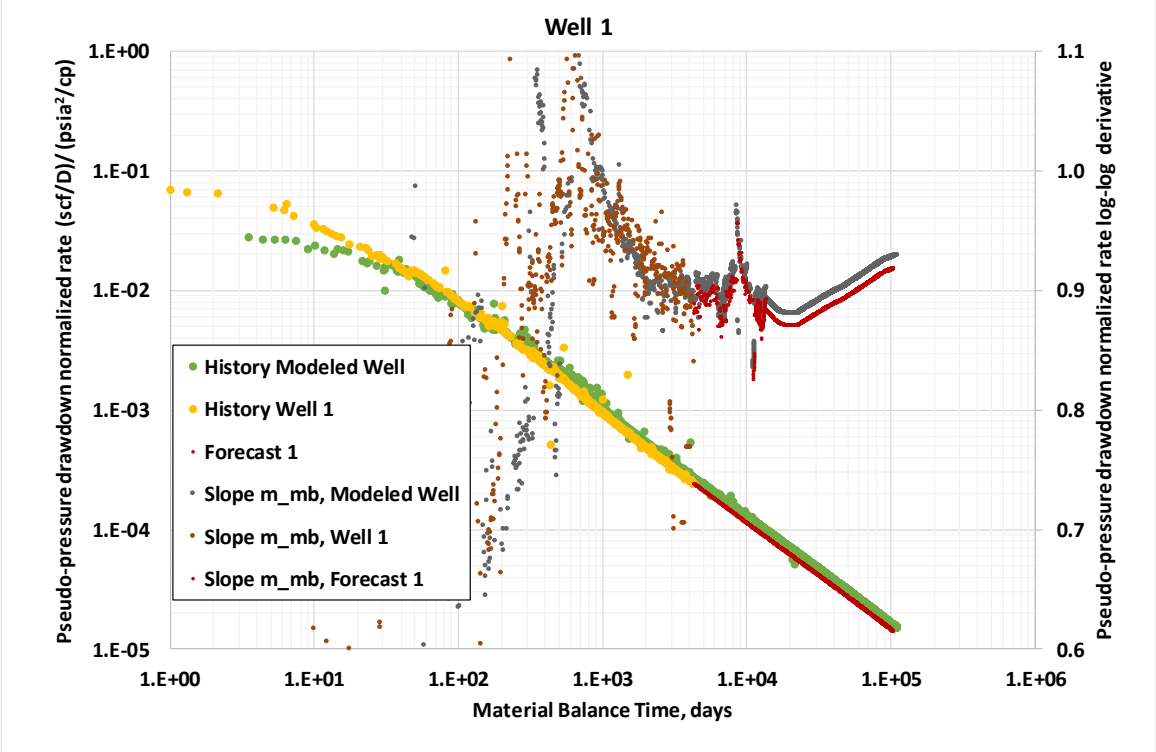

Figure 18: Well 1 log-log plot with forecast 1 m_{mb} and $q/\Delta p_p$.

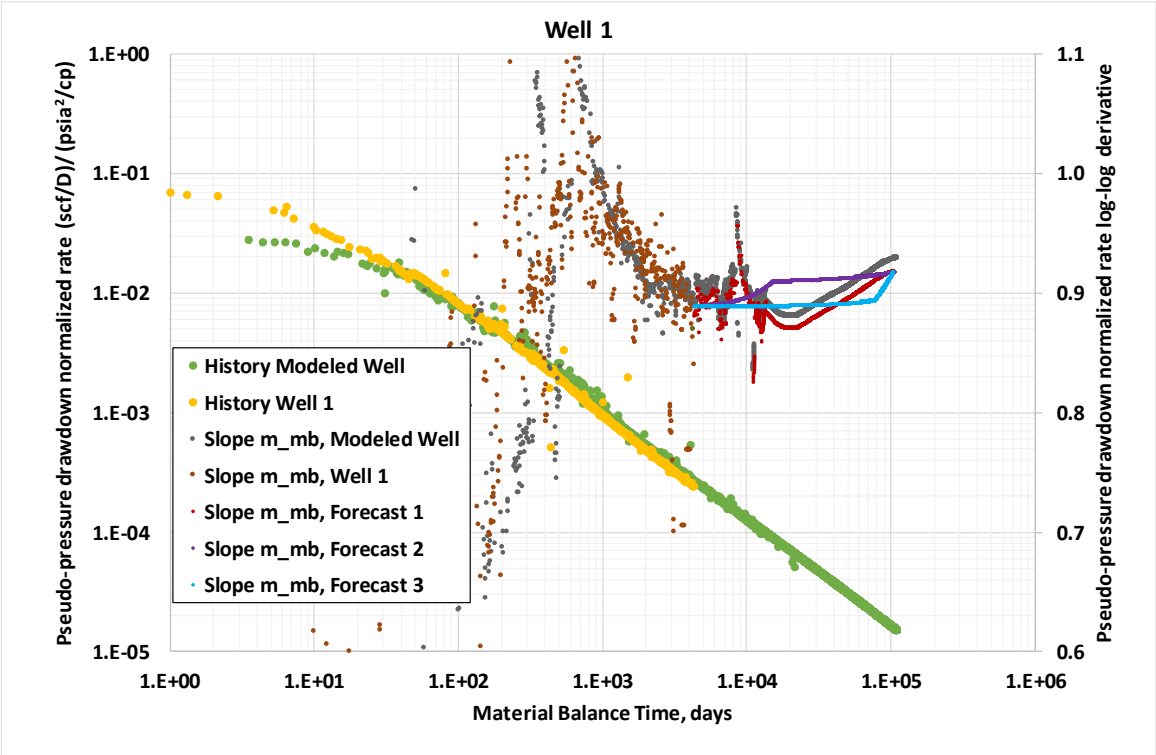

Figure 19: Well 1 log-log plot with forecast slopes m_{mb} 1,2,3.

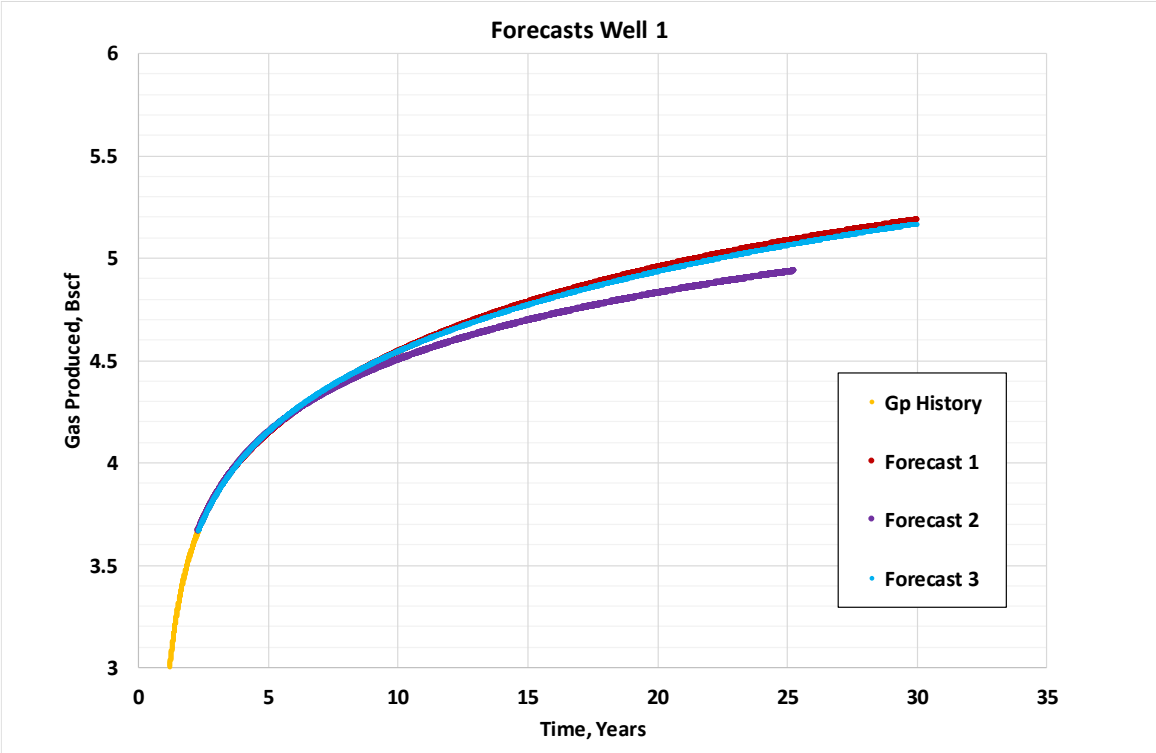

Figure 20: Well 1 forecast values of cumulative production versus time.

Table 5: Well 1 forecasts summary.

Well 1 Forecasts		
Forecast	**Production Time**	**Gp**
[#]	**[years]**	**[bscf]**
1	30	5.2
2	25.3	4.9
3	30	5.2
Num. Model	30	5.3

5.3.2 Wells 2-4

Following, log-log plots with forecast values for the derivative m_{mb}, cumulative production plots versus time and EUR tables are provided for wells 2-4. In all cases, the derivatives m_{mb} demonstrate similar behavior to the representative well. The produced forecasts are all close to the numerical model forecasts.

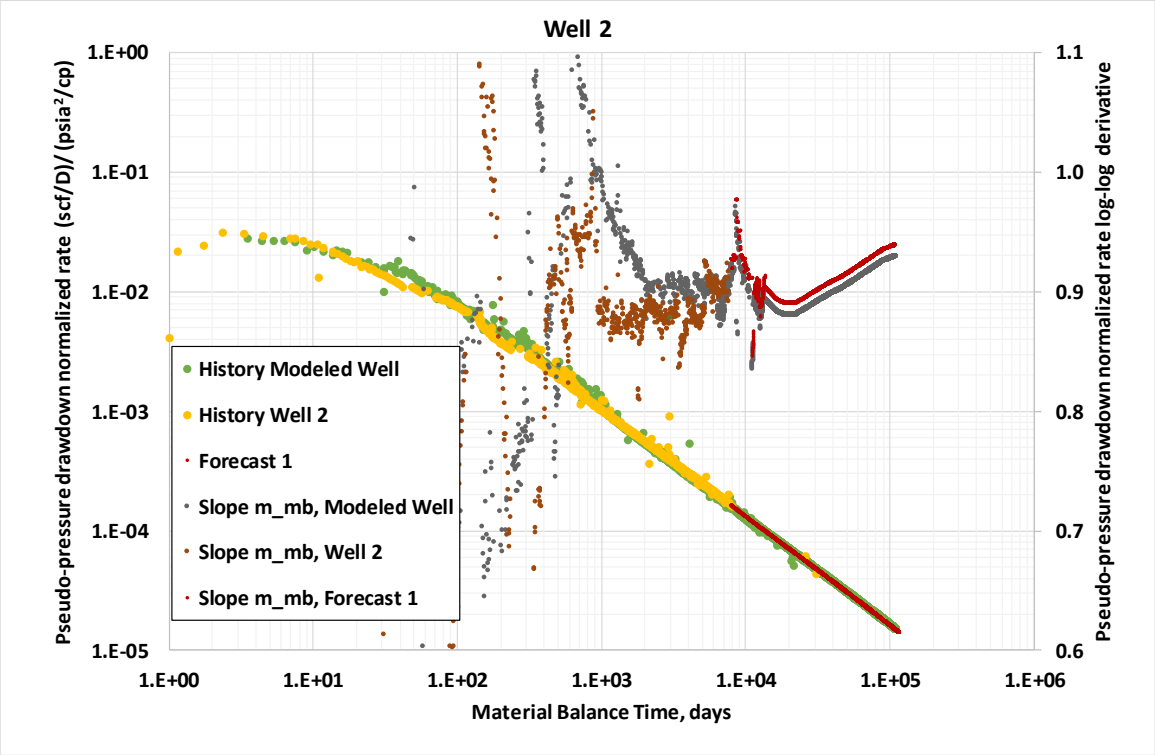

Figure 21: Well 2 log-log plot with forecast 1 m_{mb} and $q/\Delta p_p$.

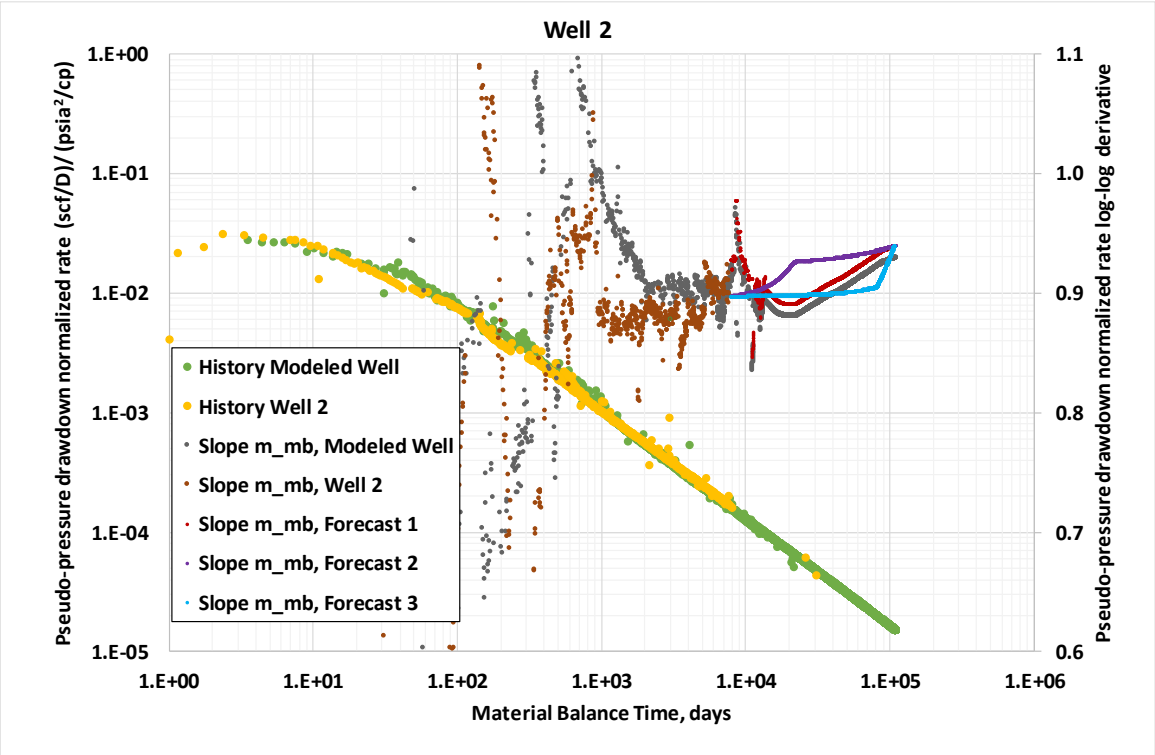

Figure 22: Well 2 log-log plot with forecast slopes m_{mb} 1,2,3.

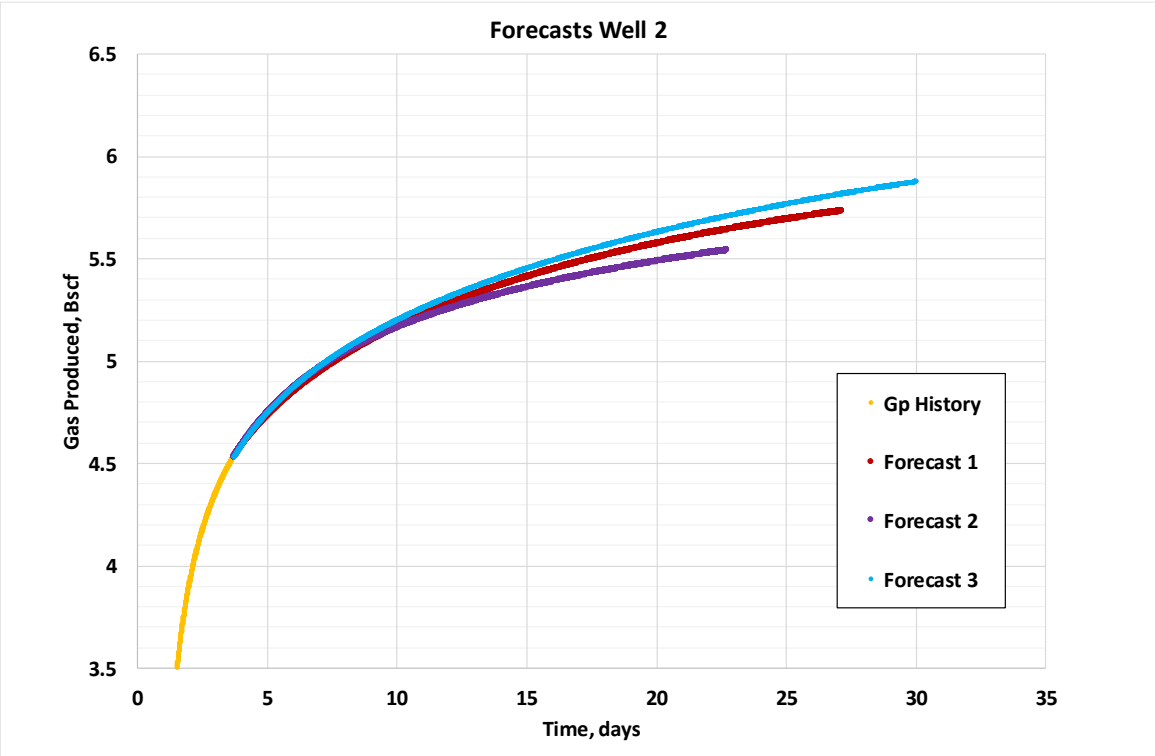

Figure 23: Well 1 forecast values of cumulative production versus time.

Table 6: Well 2 forecasts summary.

	Well 2 Forecasts	
Forecast	**Production Time**	**Gp**
[#]	**[years]**	**[bscf]**
1	27.0	5.7
2	22.7	5.5
3	30.0	5.9
Num. Model	30.0	6.0

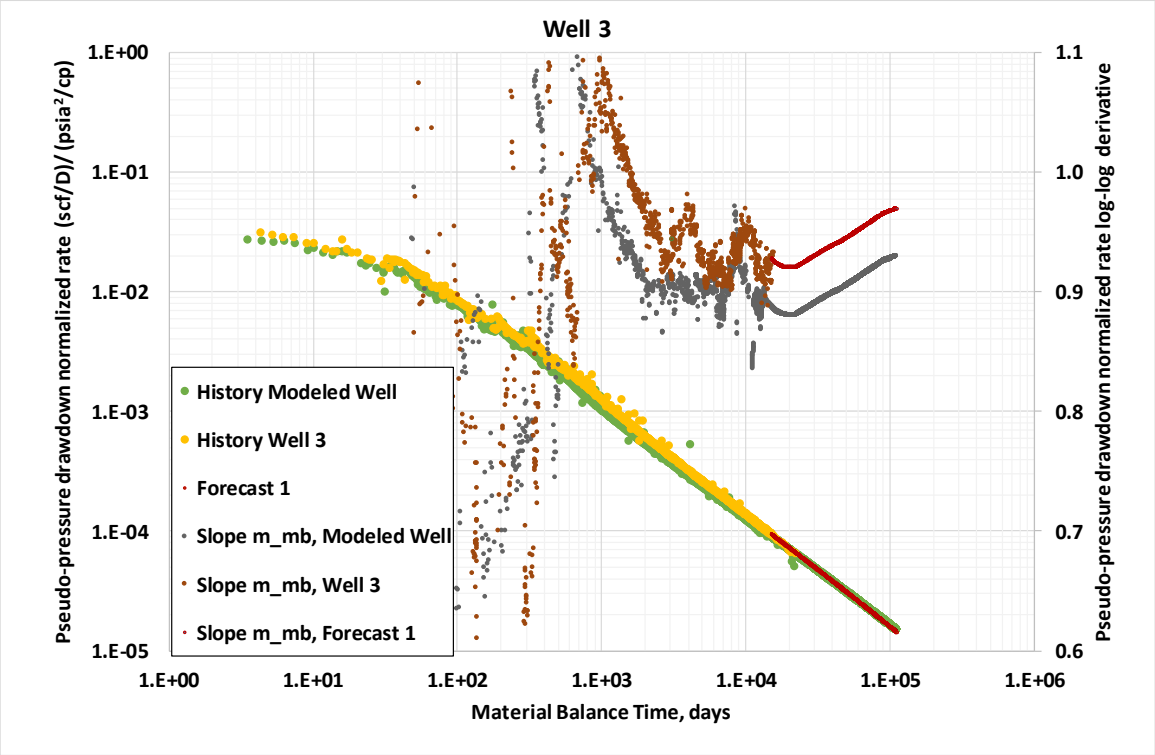

Figure 24: log-log plot of well 3 with forecast 1 m_{mb} and $q/\Delta p_p$.

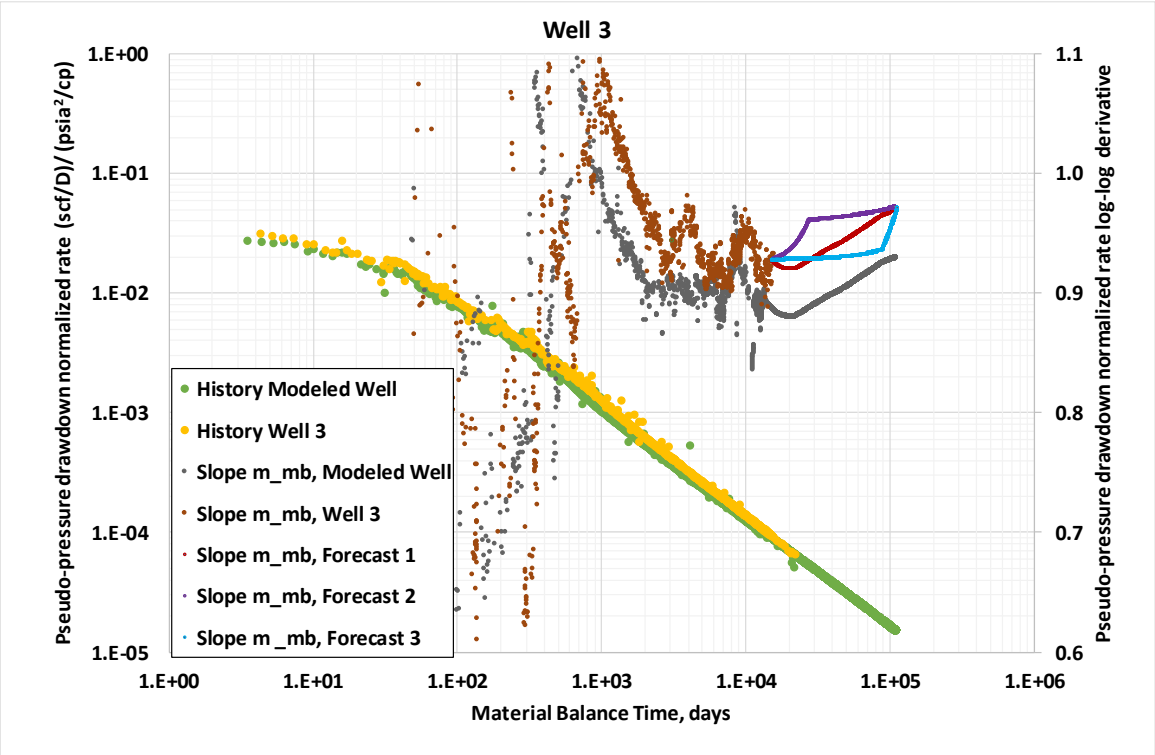

Figure 25:Well 3 log-log plot with forecast slopes m_{mb} 1,2,3.

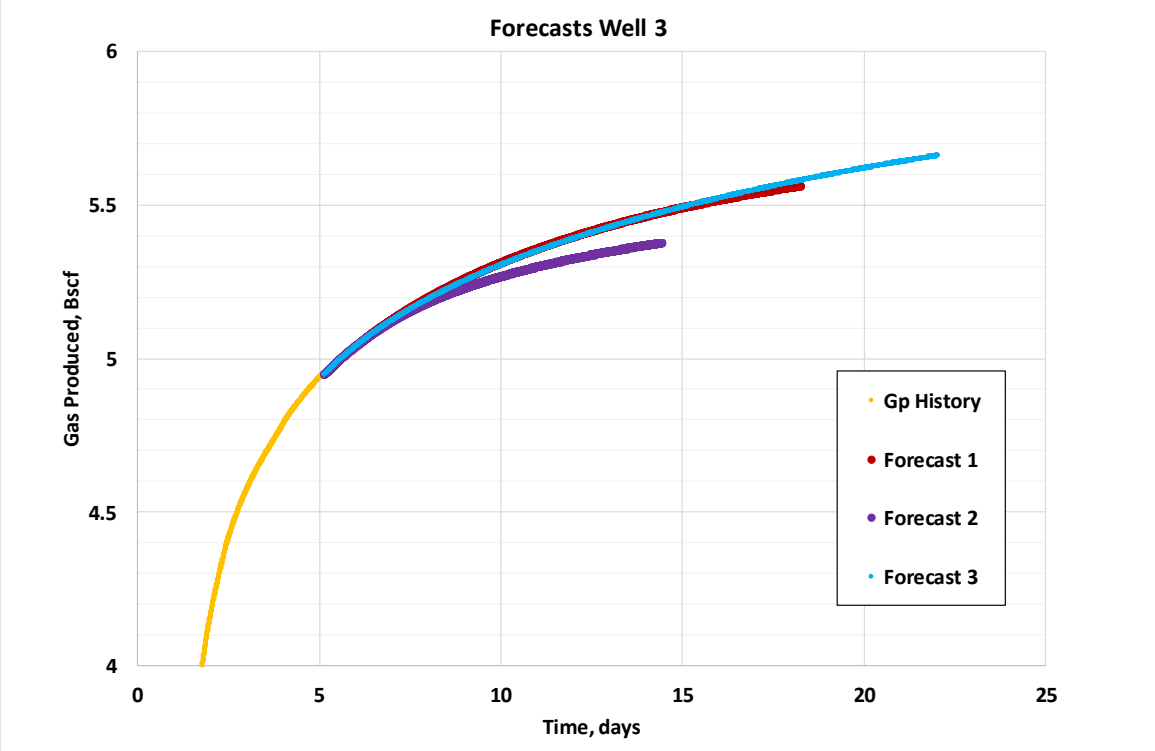

Figure 26: Well 3 forecast values of cumulative production versus time.

Table 7: Well 3 forecasts summary.

	Well 3 Forecasts	
Forecast	**Production Time**	**Gp**
[#]	**[years]**	**[bscf]**
1	18.2	5.6
2	14.4	5.4
3	22.0	5.7
Num. Model	16.3	5.5

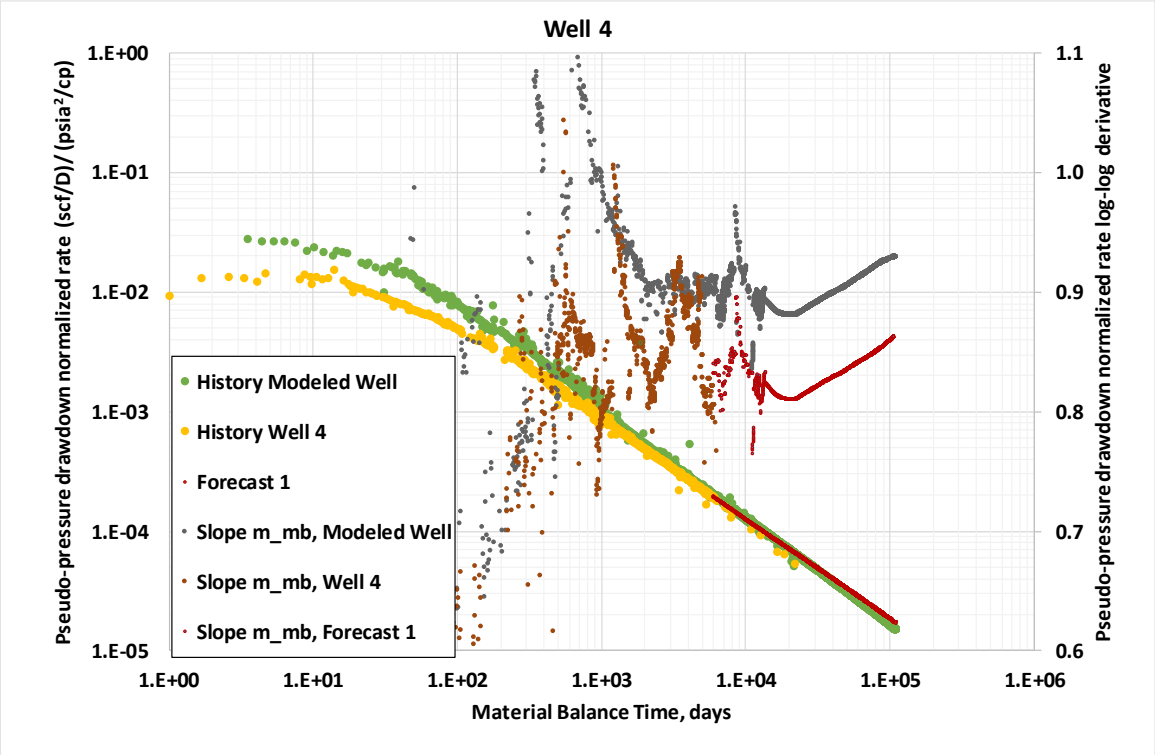

Figure 27: log-log plot of well 4 with forecast 1 m_{mb} and $q/\Delta p_p$.

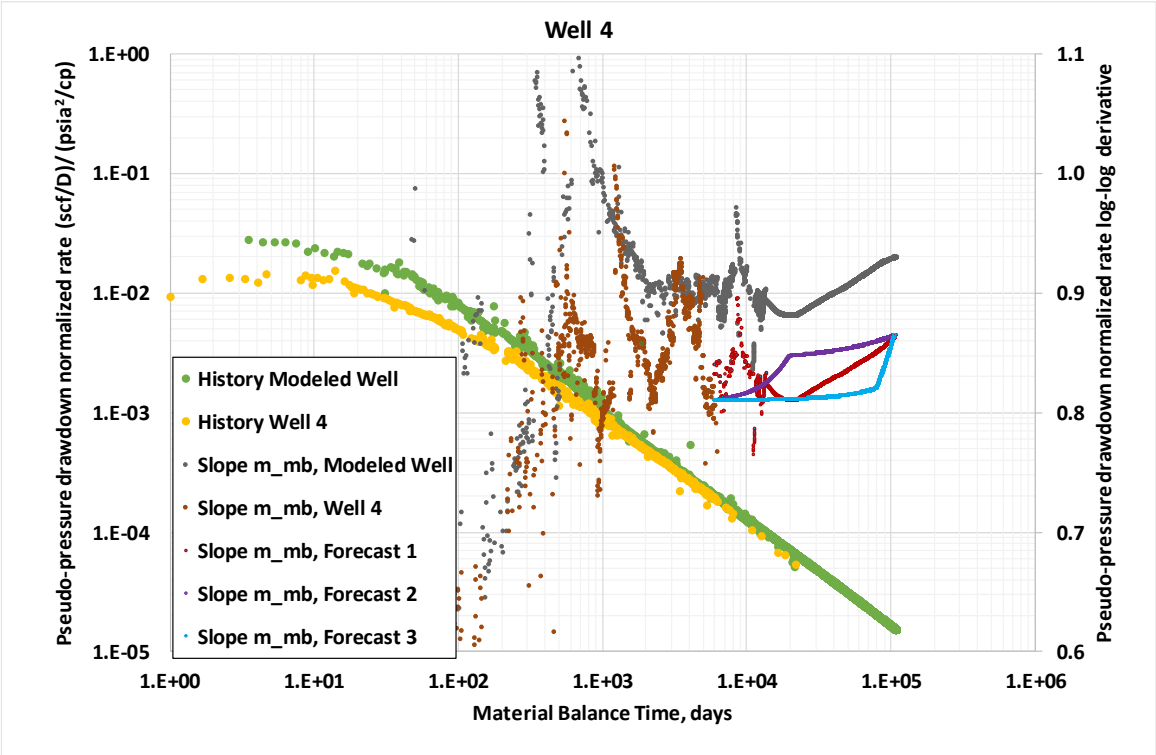

Figure 28: Well 4 log-log plot with forecast slopes m_{mb} 1,2,3.

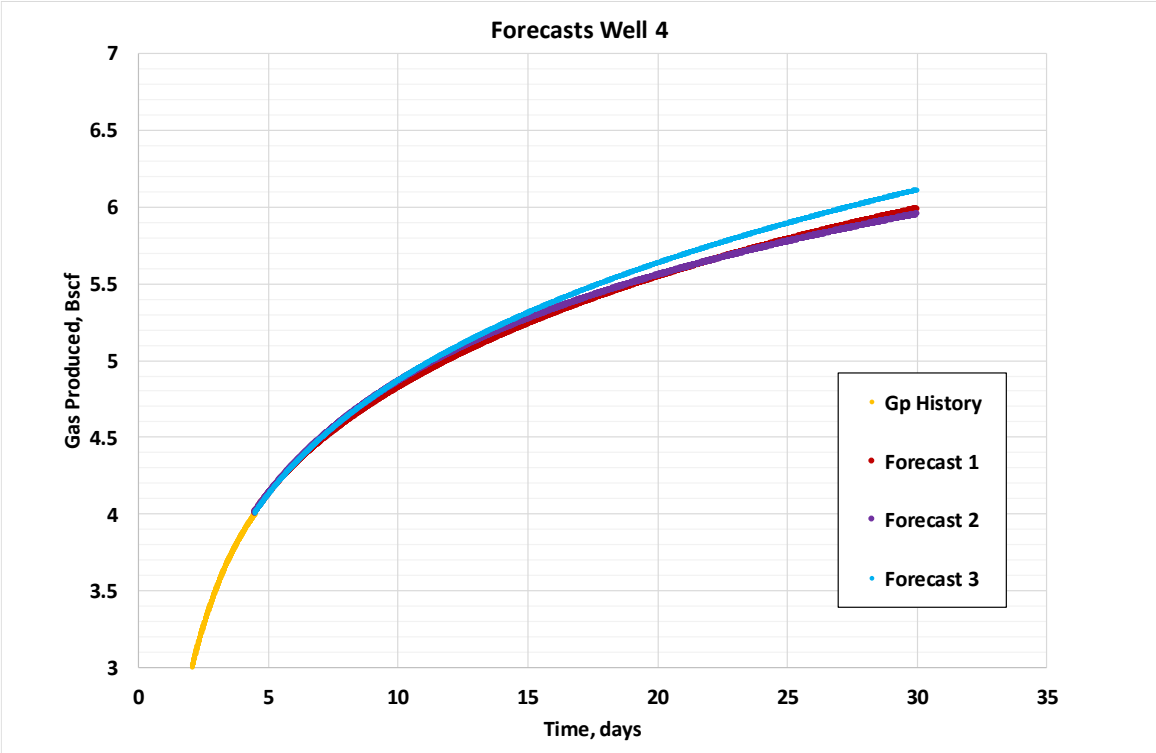

Figure 29: Well 4 forecast values of cumulative production versus time.

Table 8: Well 4 forecasts summary.

	Well 4 Forecasts	
Forecast	**Production Time**	**Gp**
[#]	**[years]**	**[bscf]**
1	30.0	6.0
2	30.0	5.9
3	30.0	6.1
Num. Model	30.0	5.9

6. Conclusions

The representative wells' forecasted signature of the derivative m_{mb} showed good ability in mass forecasting the grouped wells. It was apparent from the diagnostic plots (Log-Log plot and LIA flow plot) that the wells were behaving very similarly, which gave confidence in the forecasting. In neither of the cases were there any significant overpredictions when compared to the history-matched model forecasts for each well. The derivative m_{mb} was also shown to be a decent tool for indicating late infinite acting flow.

In the case of distinctly different performing wells, producing a history matched numerical model for each well would be the reasonable procedure. The essence of this study however, was to demonstrate that a group of wells can be forecasted in a reliable way with a single history matched well, requiring only rates and pressures.

1. The full-life signature of the representative well, which was obtained by forecasting a history-matched numerical model, succeeded in mass-producing sensible forecasts for the wells in the group.
2. The procedure was successful in identifying a unique group trend, requiring data only on production rates and tubing pressures for all wells.
3. The procedure of extending the trend of the derivative m_{mb} was simple and fast, and succeeded in capturing transient contribution while still being constrained by the representative wells' history matched model performance trend.

The data in this work is limited to five wells producing from the same formation. A more thorough research, comprising more wells could be performed. Further, the inclusion of several good history matches for the representative well, instead of only one, could be done in order to grasp the whole spectrum of possible forecast figures. Another study would be to quantify how much the well, reservoir and completion parameters in the group can differ, while still produce reasonable forecasts.

7. References

- Al-Hussainy, R., Ramey, H. J., & Crawford, P. B. (1966, May 1). The Flow of Real Gases Through Porous Media. Society of Petroleum Engineers. doi:10.2118/1243-A-PA
- Anderson, D.M., Stotts, G.W.J., Mattar, L., Ilk, D., and Blasingame, T.A., "Production Data Analysis-Challenges, Pitfalls, Diagnostics", paper SPE 102048, presented at the SPE Annual Technical Conference and Exhibition, 24-27 September, San Antonio, TX, 2006.
- Anderson, Nobakht, Moghadam, Mattar, Fekete Associates Inc., "Analysis of Production Data From Fractured Shale Gas Wells", paper SPE 131787, Presented at the SPE Unconventional Gas Conference, Pittsburgh, PA, 23-25 February 2010
- Arps, J. J. (1945, December 1). Analysis of Decline Curves. Society of Petroleum Engineers. doi:10.2118/945228-G
- Bourdet, D., Ayoub, J.A., and Pirard, Y.M. 1989. Use of Pressure Derivative in Well-Test Interpretation. SPEFE 4 (2): 228- 293-302
- Brooks, R.H. and Corey, A.T. 1964. Hydraulic Properties of Porous Media. Hydrology Papers, No. 3, Colorado State U., Fort Collins, Colorado.
- Collins, P.W., Ilk, D. DeGoyler, McNaughton, "Practical Considerations for Production Forecasting in Unconventional Reservoir Systems – Processing of Large Group of Wells Using Production Diagnostics and Model-Based Analysis", paper SPE 174984-MS, presented at the SPE Annual Technical Conference and Exhibition held in Houston, TX, USA, 28-30 September 2015
- Fetkovich, M. J. (1980, June 1). Decline Curve Analysis Using Type Curves. Society of Petroleum Engineers. doi:10.2118/4629-PA
- Fetkovich, M. J., Fetkovich, E. J., & Fetkovich, M. D. 1996. Useful Concepts for Decline Curve Forecasting, Reserve Estimation, and Analysis. Society of Petroleum Engineers. doi:10.2118/28628-PA
- Fetkovich, M. J., & Vienot, M. E. (1984, December 1). Rate Normalization of Buildup Pressure By Using Afterflow Data. Society of Petroleum Engineers. doi:10.2118/12179-PA
- Golan M. and Whitson C.H.: "Well Performance", (1987).

- Gray, H.E.: “Vertical Flow Correlation in Gas Wells”, User’s Manual for API 14B Surface Controlled Subsurface Safety Valve Sizing Computer Program, 2nd Edition, (Appendix B), American Petroleum Institute, Dallas, TX, June 1978
- Ibrahim, M. H., & Wattenbarger, R. A. (2006, January 1). Analysis of Rate Dependence in Transient Linear Flow in Tight Gas Wells. Society of Petroleum Engineers. doi:10.2118/100836-MS
- Ilk, D., Rushing, J.A., Perego A.D., et al. 2008. Exponential vs. Hyperbolic Decline in Tight Gas Sands: Understanding the Origin and Implications for Reserve Estimates Using Arps' Decline Curves. Paper SPE 116731 presented at the SPE Annual Technical Conference and Exhibition, Denver, CO, 21−24 September
- Lee, A.L. et al.: "The Viscosity of Natural Gases," JPT(Aug. 1966) 997-1001; Trans., AIME, 237.
- Nystad, M., Analysis of Linear Gas Flow in Unconventional Reservoirs, NTNU, 2015.
- Palacio, J.C., Blasingame, T.A., “Decline-Curve Analysis Using Type Curves—Analysis of Gas Well Production Data
- Pratikno, H., ConocoPhillips, Reese, D.E., Consultant, Summers, L.E., ConocoPhillips, “Hyperbolic Decline Parameters During and After Linear Flow: Field Example from the Barnett Shale Using Public Data”, paper SPE 171568-MS, Presented at the SPE/CSUR Unconventional Resources Conference – Calgary, Alberta, Canada, 30 September – 2 October 2014
- Sutton, R.P.: “Compressibility Factors for High-Molecular Weight Reservoir Gases,” paper SPE 14265 presented at the 1985 SPE Annual Technical Conference and Exhibition, Las Vegas, Nevada, 22–25 September.
- Wattenbarger, R. A., El-Banbi, A. H., Villegas, M. E., & Maggard, J. B. (1998, January 1). Production Analysis of Linear Flow Into Fractured Tight Gas Wells. Society of Petroleum Engineers. doi:10.2118/39931-MS
- Whitson, NTNU, Coll, BG Group, Majzoub Dahouk, Juell, Petrostreamz AS, “Shale Reserve Forecasting – Model Consistency and Uncertainty”, paper SPE 180140-MS, presented at the SPE Europec featured at 78th EAGE Conference and Exhibition held in Vienna, Austria, 30 May–2 June 2016.

8. Nomenclature

- b = Arps hyperbolic rate equation exponent, dimensionless
- D = Arps Nominal Decline
- D_D = Dimensionless Drawdown, dimensionless
- D_i = Arps Initial Nominal Decline
- μ_g = gas viscosity, cp
- μ_{gi} = gas viscosity at initial reservoir pressure, cp
- c_g = gas compressibility, psi^{-1}
- c_{ti} = total compressibility at initial conditions, psi^{-1}
- f_{cp} empirical correction factor, dimensionless
- h = net formation thickness, ft
- k = rock permeability, md
- m_{LF} = slope of linear flow diagnostic plot
- m_{mb} = value of log-log derivative of pseudo-pressure drawdown normalized rate to material balance time
- m_{PSS} = stabilized slope of Log-Log diagnostic plot
- η = hydraulic diffusivity term, $md/(cp*psia^{-1})$
- p_D = dimensionless pressure
- p_{Dc} = dimensionless pressure constant
- p_i = initial reservoir pressure, psia
- p_p = Pseudo-Pressure, $psia^2/cp$
- p_{pi} = real gas pseudo-pressure at Initial Conditions, $psia^2/cp$
- p_{pwf} = real gas pseudo-pressure at current flowing pressure, $psia^2/cp$
- p_{wf} = bottomhole flowing pressure, psia
- Q = cumulative production, Mscf
- q_g = surface gas rate, Mscf/D
- q_i = Arps initial production rate, Mscf/D
- t = time, D

- t_{Dxf} = dimensionless time for a planar fracture geometry
- t_{Dxfc} = dimensionless time constant for a planar fracture geometry
- t_{LS} = linear superposition time, $D^{0.5}$
- t_{mb} = material balance time, D
- T_r = reservoir temperature, °R
- x_f = half-fracture length, ft
- y_e distance from fracture to no-flow boundary, ft
- φ = rock porosity, fraction

9. Abbreviations

EUR = Estimated Ultimate Recovery

OGIP = Original Gas-in-place

LIA = Linear Infinite Acting

PSS = Pseudo-Steady State

BD = Boundary-Dominated